Recent results from High Energy Stereoscopic System (H.E.S.S.)

Rafał Moderski

Nicolaus Copernicus Astronomical Center

High Energy Stereoscopic System – H.E.S.S.

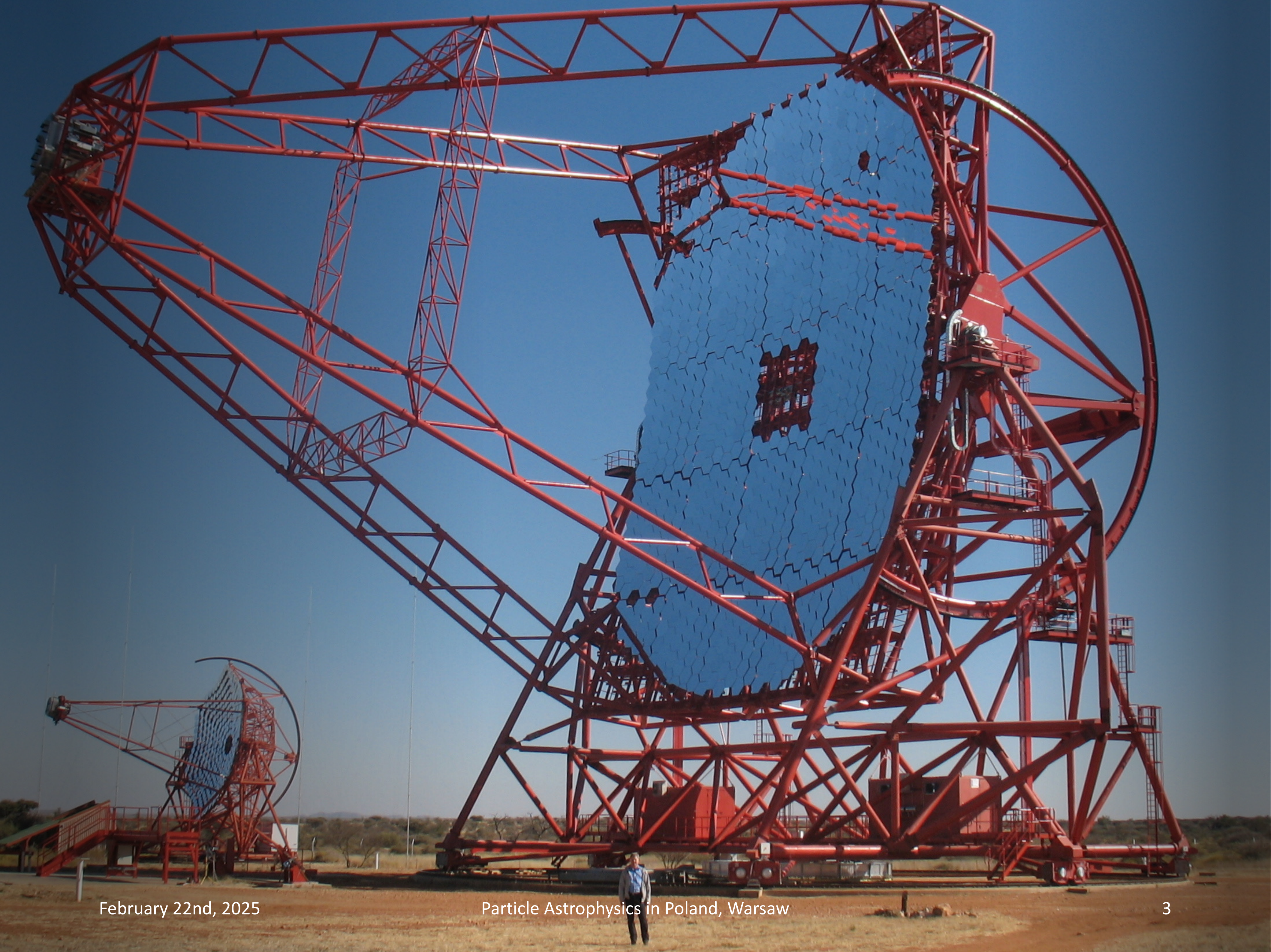

H.E.S.S. - basic data

– **High Energy Stereoscopic System**;
– **five telescopes** 120 m x 120 m area;
– **4 x 12 m diameter** spherical main mirror f=13 m, 362 circular mirror facets 60 cm diameter, 4 x 107m^2 collecting area, camera: 960 vacuum tube photo-multipliers, field of view ~5°; 1ns sampling;
– **1 x 28 m diameter** parabolic mirror f=36 m, 614 m^2 area, 875 hexagonal mirror facets 90 cm (flat-to-flat), camera: 2048 photo-multipliers, 1 ns sampling, field of view ~3.2^{O}, 2.8 t
– duty cycle ~1000h/yr (moonless nights required);
– **energy range: ~30GeV - >10TeV**
– **resolution: angular – 0.1°, energetic – 15% @ 1TeV**
– **sensitivity: 1% Crab (5σ, 25h)**

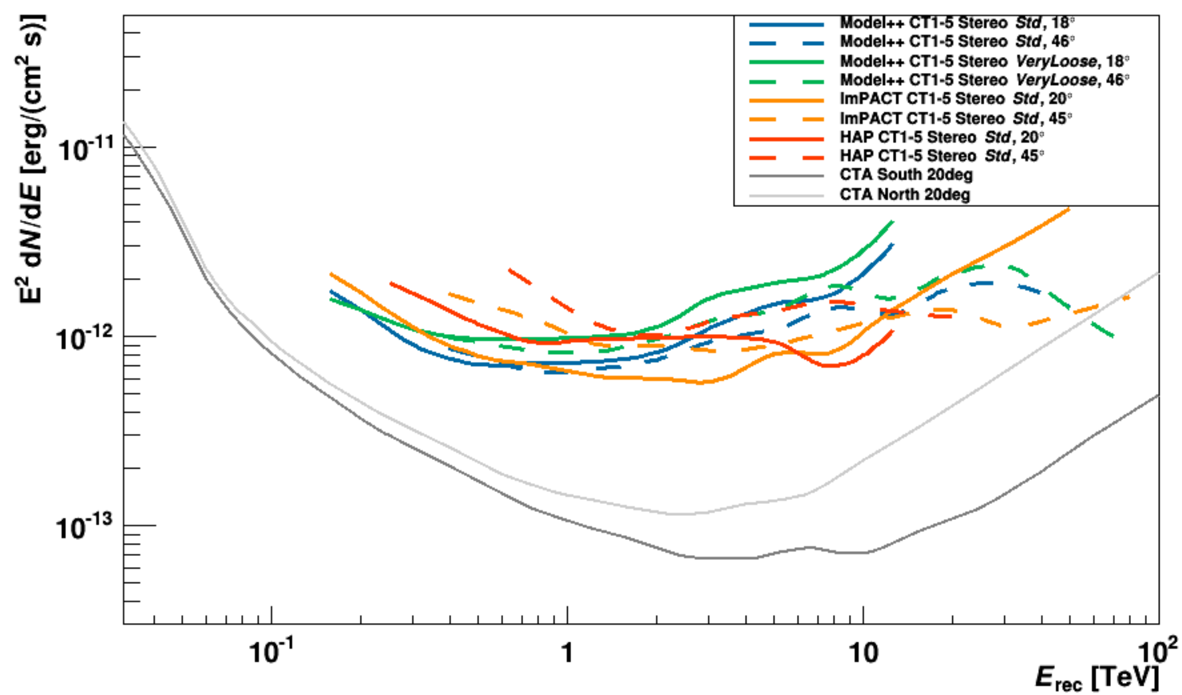

aw

HESS Collaboration

>12 countries, >30 scientific institutions, >100 scientists

Max-Planck-Institut für Kernphysik, Heidelberg, Germany
Humboldt Universität Berlin, Germany, Institut für Physik
Ruhr-Universität Bochum, Germany, Fakultät für Physik und Astronomie
Universität Erlangen-Nürnberg, Germany, Physikalisches Institut
Universität Hamburg, Germany, II. Institut für Experimentalphysik
Landessternwarte Heidelberg, Germany
Universität Tübingen, Germany, Institut für Astronomie und Astrophysik (IAAT)
Laboratoire Leprince-Ringuet (LLR), Ecole Polytechnique, Palaiseau, France
LPNHE, Universités Paris VI - VII, France,
APC, Paris, France
CEA Saclay, France
Observatoire de Paris-Meudon, DAEC, France
LAPP Annecy, France
Université de Grenoble, France
LPTA, Université Montpellier II, France
CERS, Toulouse, France
Durham University, U.K.
University of Leeds, School of Physics and Astronomy
Dublin Institute for Advanced Studies, Dublin, Ireland

Nicolaus Copernicus Astronomical Center, Polish Academy of Sciences, Warsaw, Poland
W. Kluźniak, R. Moderski, B. Rudak, A. Zdziarski
Astronomical Observatory, Jagiellonian University, Cracow, Poland
M. Ostrowski, Ł. Stawarz
Institute of Nuclear Physics, Polish Academy of Sciences, Cracow, Poland
J. Niemiec, A. Wierzcholska, S. Cassanova
Astronomical Observatory, University of Warsaw, Poland
T. Bulik
Center for Astronomy, Nicolaus Copernicus University, Toruń, Poland
K. Katarzyński

Charles University, Prag, Czech Republic, Nuclear Center
Yerevan Physics Institute, Yerevan, Armenia
University of Adelaide, Australia, School of Chemistry and Physics
University of Namibia, Windhoek, Namibia
North West University, Republic of South Africa

Cherenkov technique

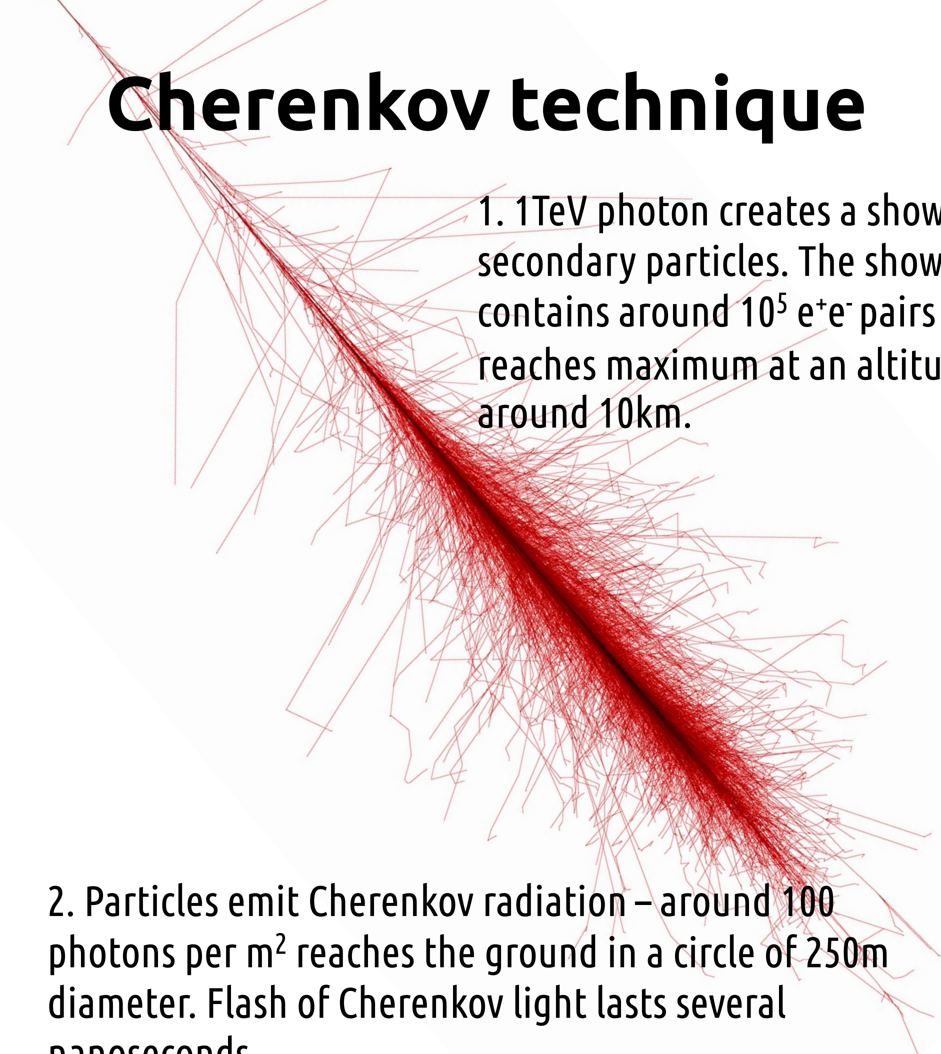

1. 1TeV photon creates a shower of secondary particles. The shower contains around 10^5 e^+e^- pairs and reaches maximum at an altitude of around 10km.

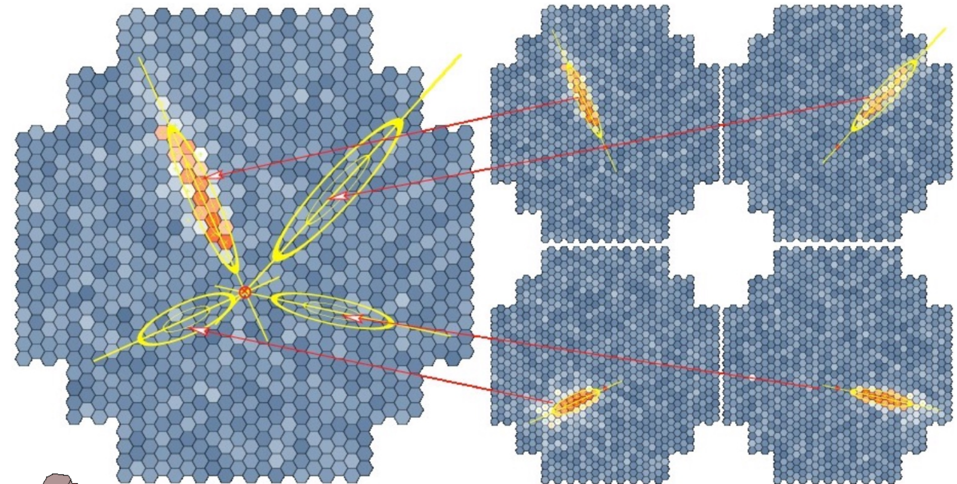

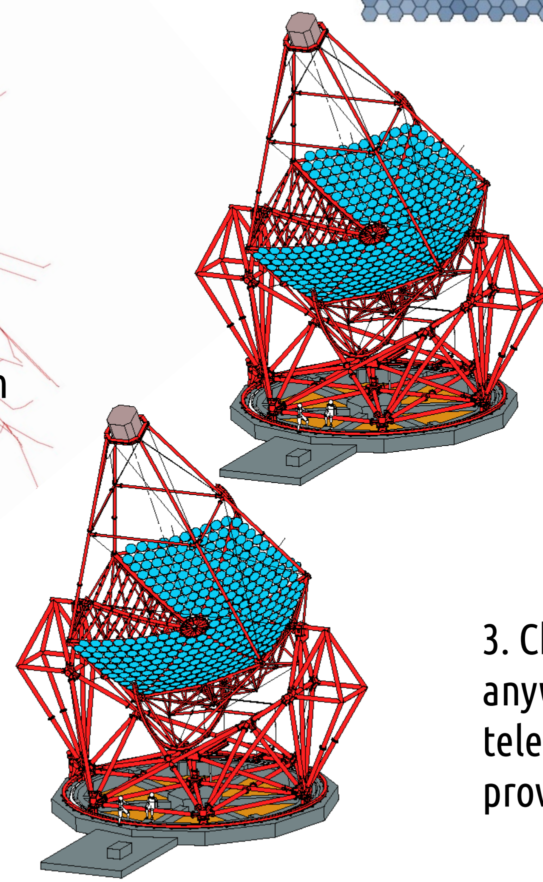

4. Image of the air shower is captured by the camera.

2. Particles emit Cherenkov radiation – around 100 photons per m^2 reaches the ground in a circle of 250m diameter. Flash of Cherenkov light lasts several nanoseconds.

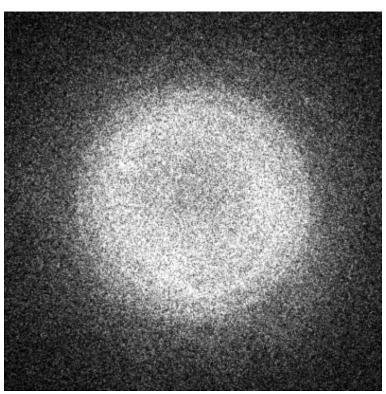

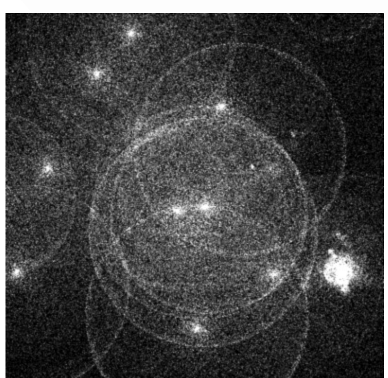

3. Cherenkov photons can be registered anywhere within the cone by an optical telescope (if enough sensitive) – this provides an effective area of **50000 m^2**

Hardware upgrades

– all CT1-CT4 cameras upgraded in 2017 to CT1U-CT4U: new electronics (NeCTAr chip), new light collectors, new ventilation system

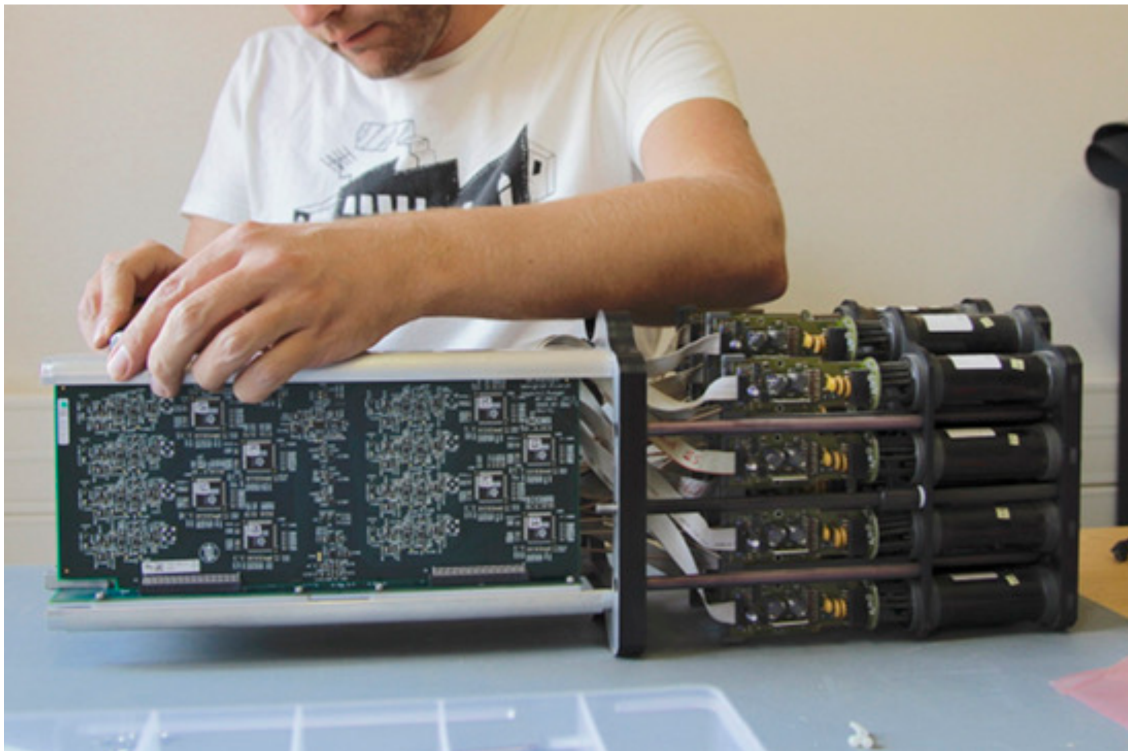

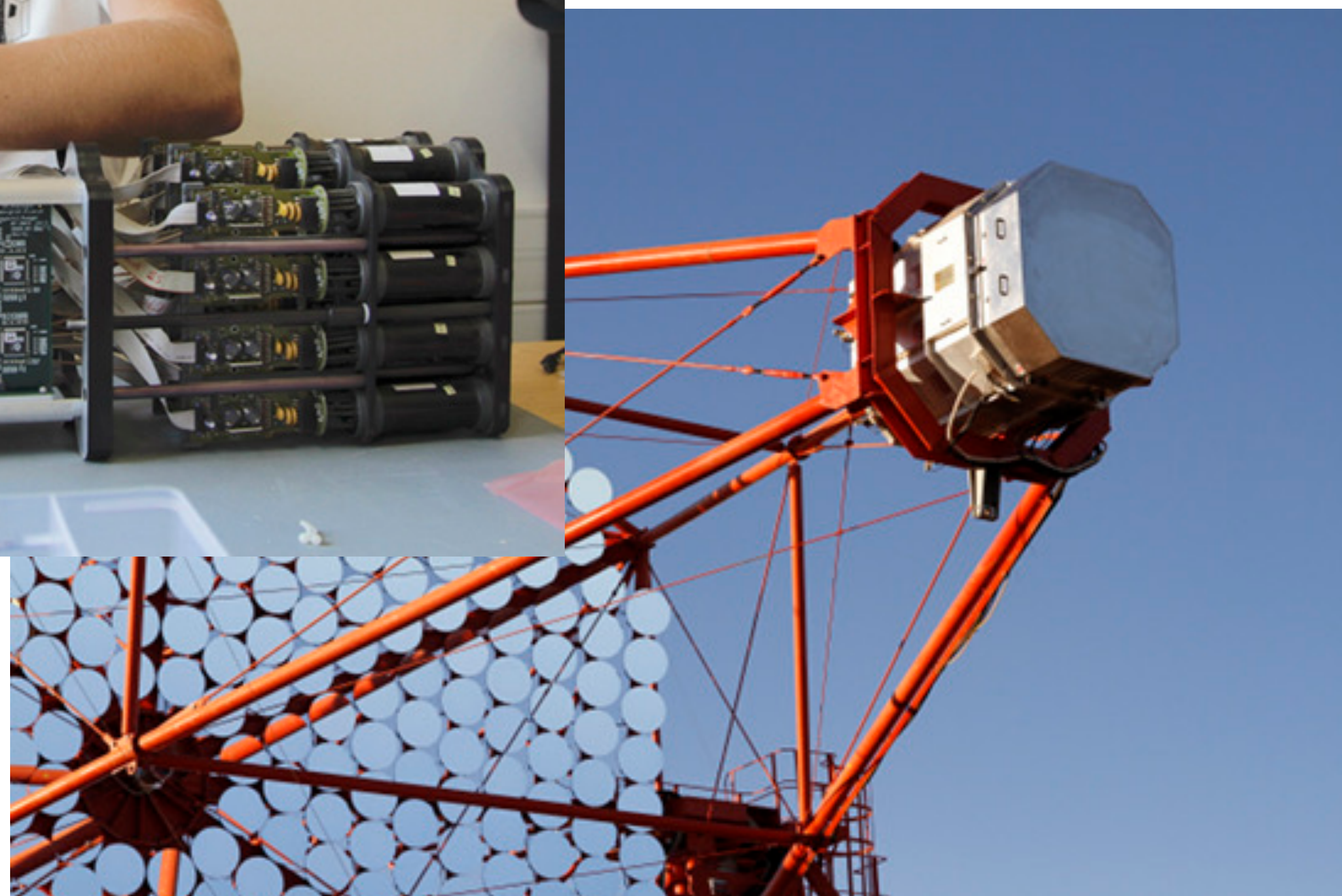

Hardware upgrades

– Data Acquisition System (DAQ) upgraded in 2019

– CT5U upgrade in Oct 2019 – completely new camera based on FlashCAM design (full digital readout)

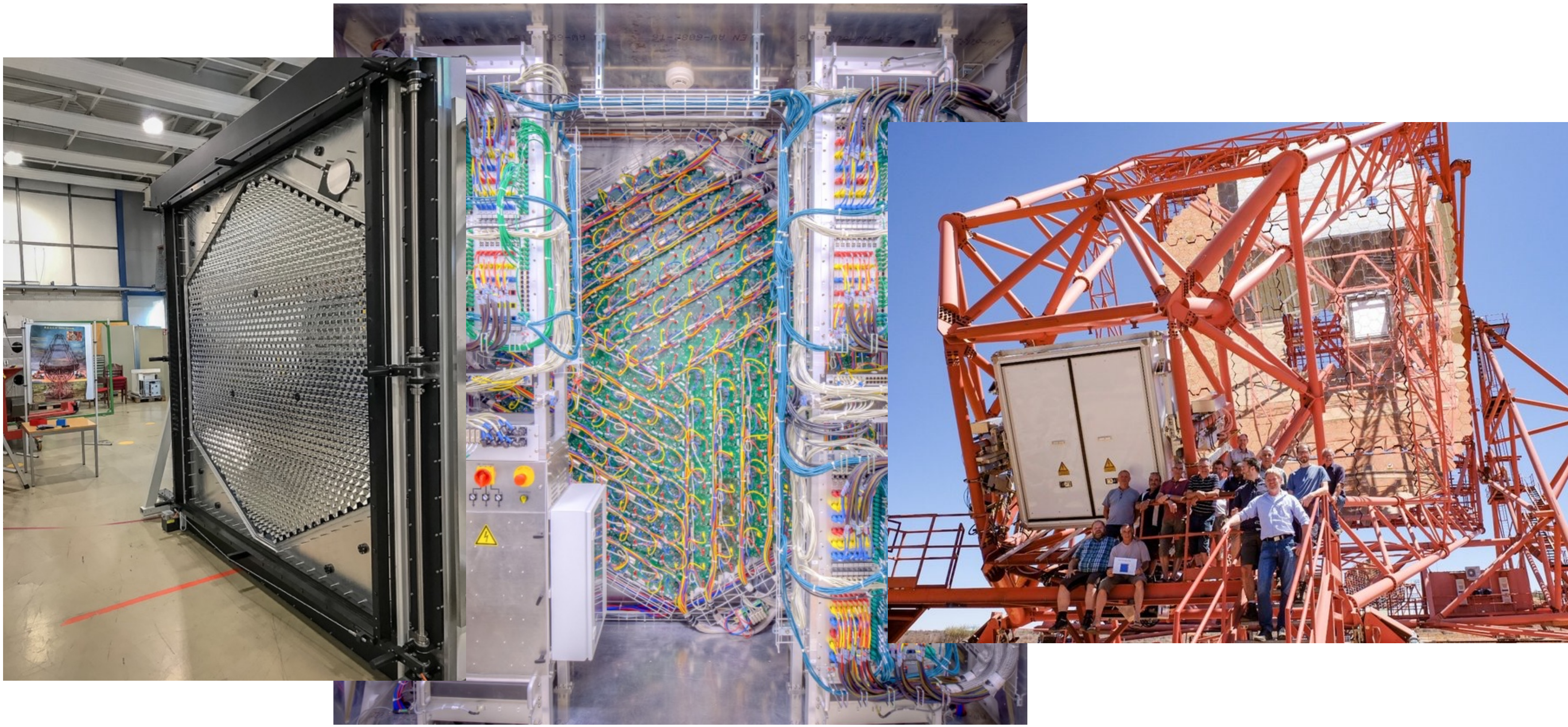

H.E.S.S. as a pathfinder project for CTA

Particle astrophysics research

Galactic sources:

- supernova remnants (SNRs),
- pulsars and pulsar wind nebulae (PWNs),
- star clusters,
- Galactic centre,
- X-ray binaries (XRBs) and microquasars.

Extragalactic sources:

- active galactic nuclei (AGNs),
- dwarf galaxies (DSs),
- extragalactic background light (EBL),
- gamma-ray bursts (GRBs),
- clusters of galaxies.

Multi-wavelength and multi-messenger observations.

Fundamental physics:

- origin of **cosmic-rays (CR)**
- dark matter (DM),
- Lorentz invariance violation (LIV),

Physical processes:

- particle acceleration to the highest energies (CR),
- particle and radiation propagation in the intergalactic medium,
- structure of the magnetic field at different scales,
- radiation production mechanisms at high energy.

H.E.S.S. - some results

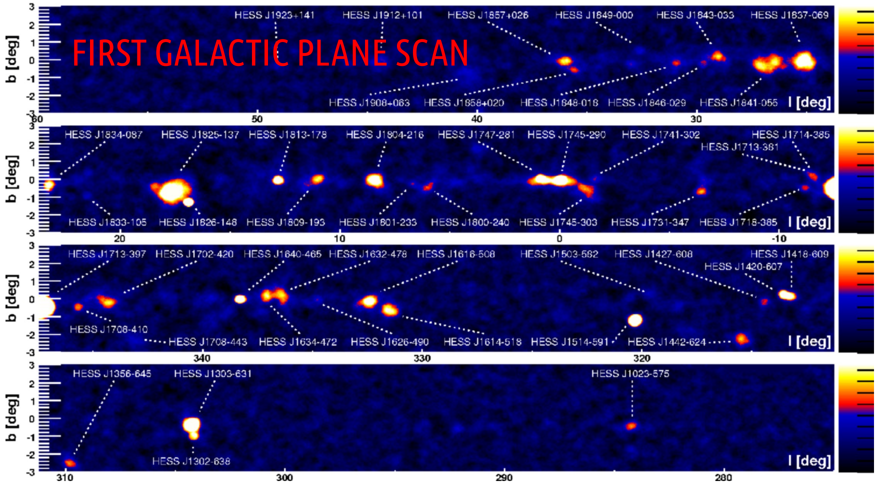

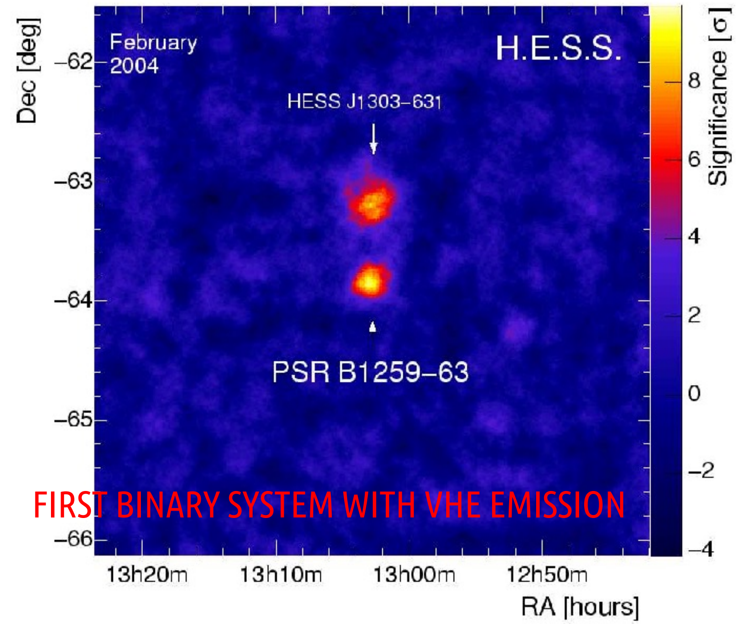

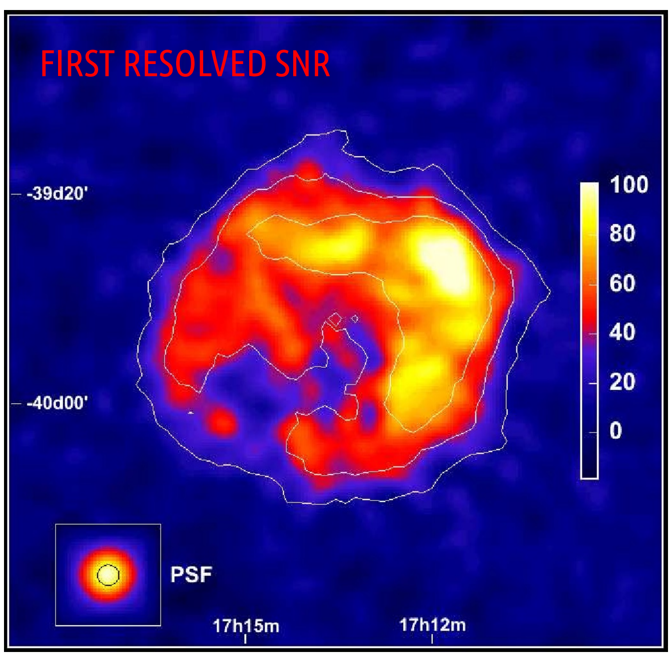

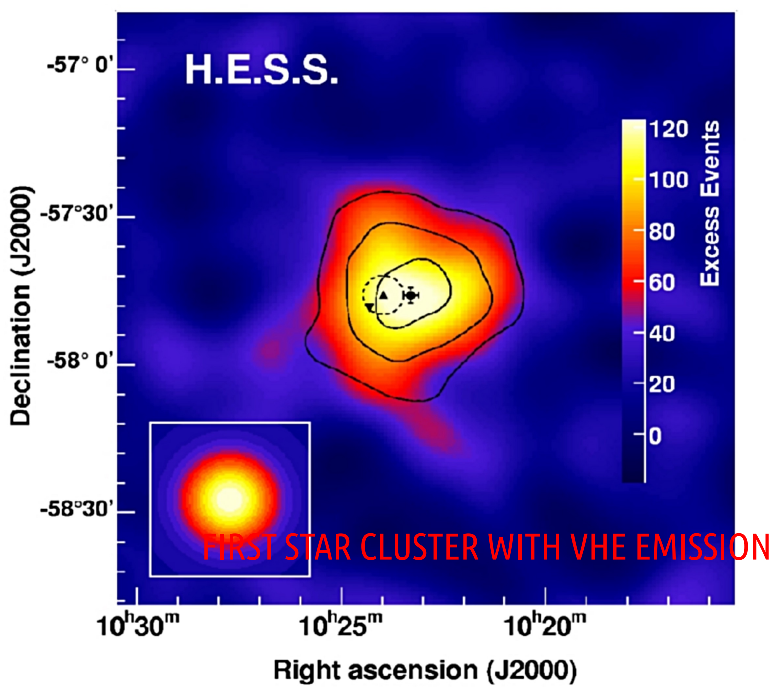

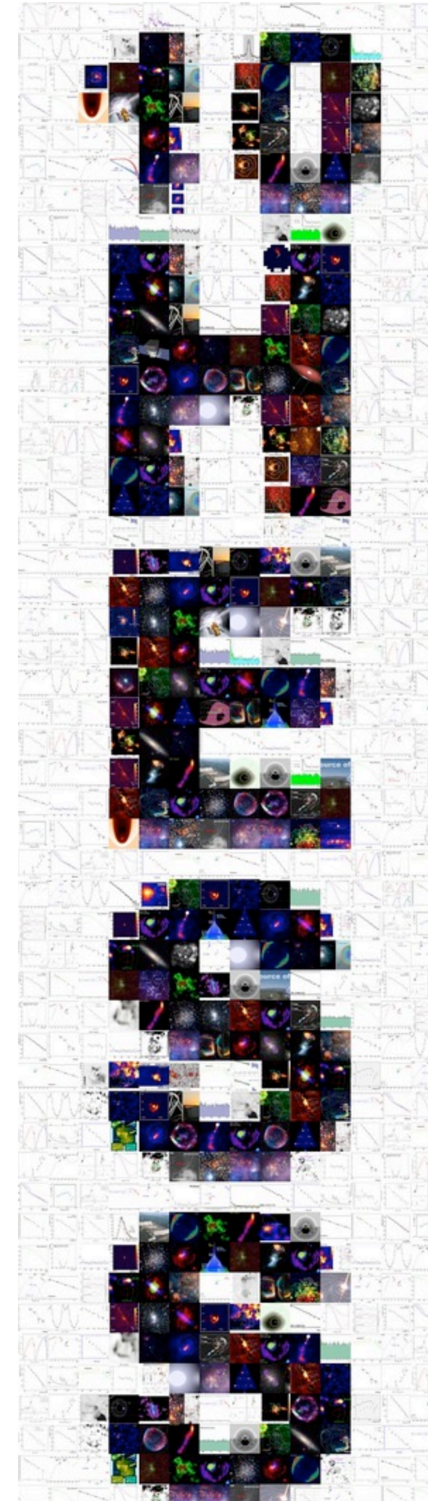

H.E.S.S. Galactic Plane Survey – HGPS

*H.E.S.S. Collaboration, A&A **612**, A1 (2018)*

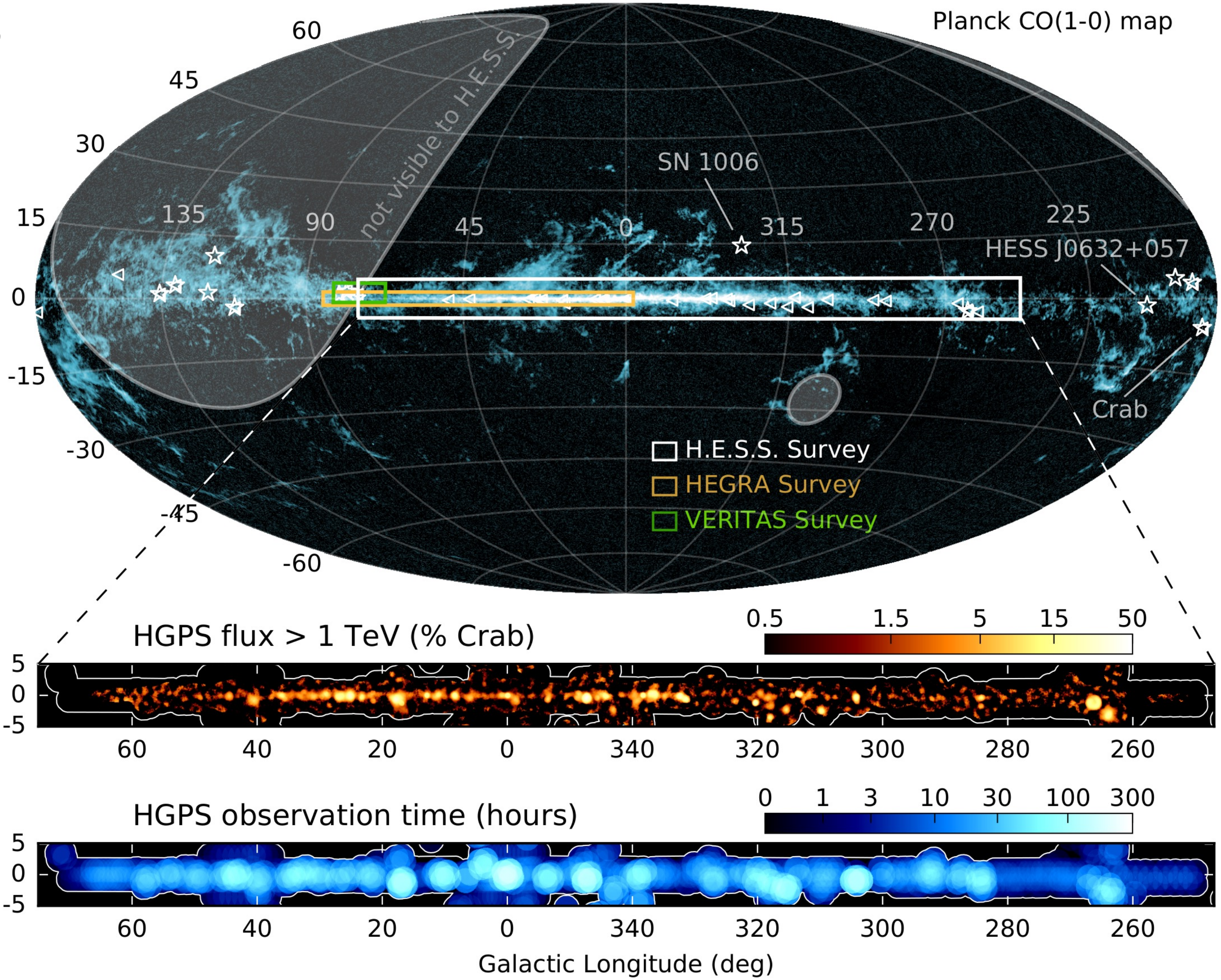

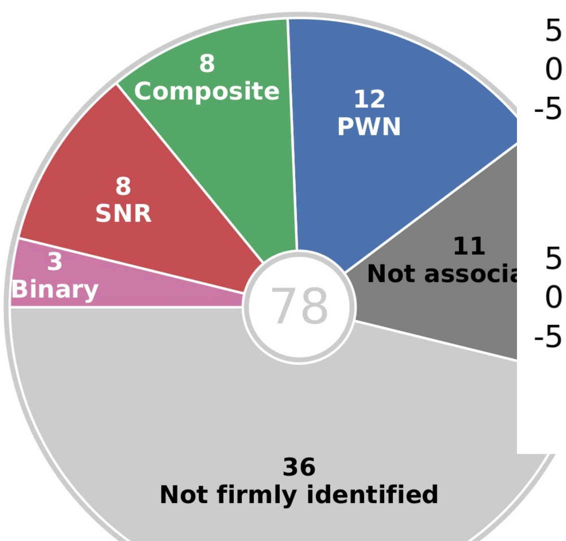

HGPS and HAWC

– In the part of the Galactic plane common to H.E.S.S. and HAWC, four HAWC sources previously undetected by H.E.S.S. show significant emission above the detection level of 5σ

– a consistent view of the γ-ray sky between WCD and IACT techniques

– The future observatories SWGO (Southern Wide-field Gamma-ray Observatory and CTA (Cherenkov Telescope Array) can take advantage of the complementarity of the two detection techniques

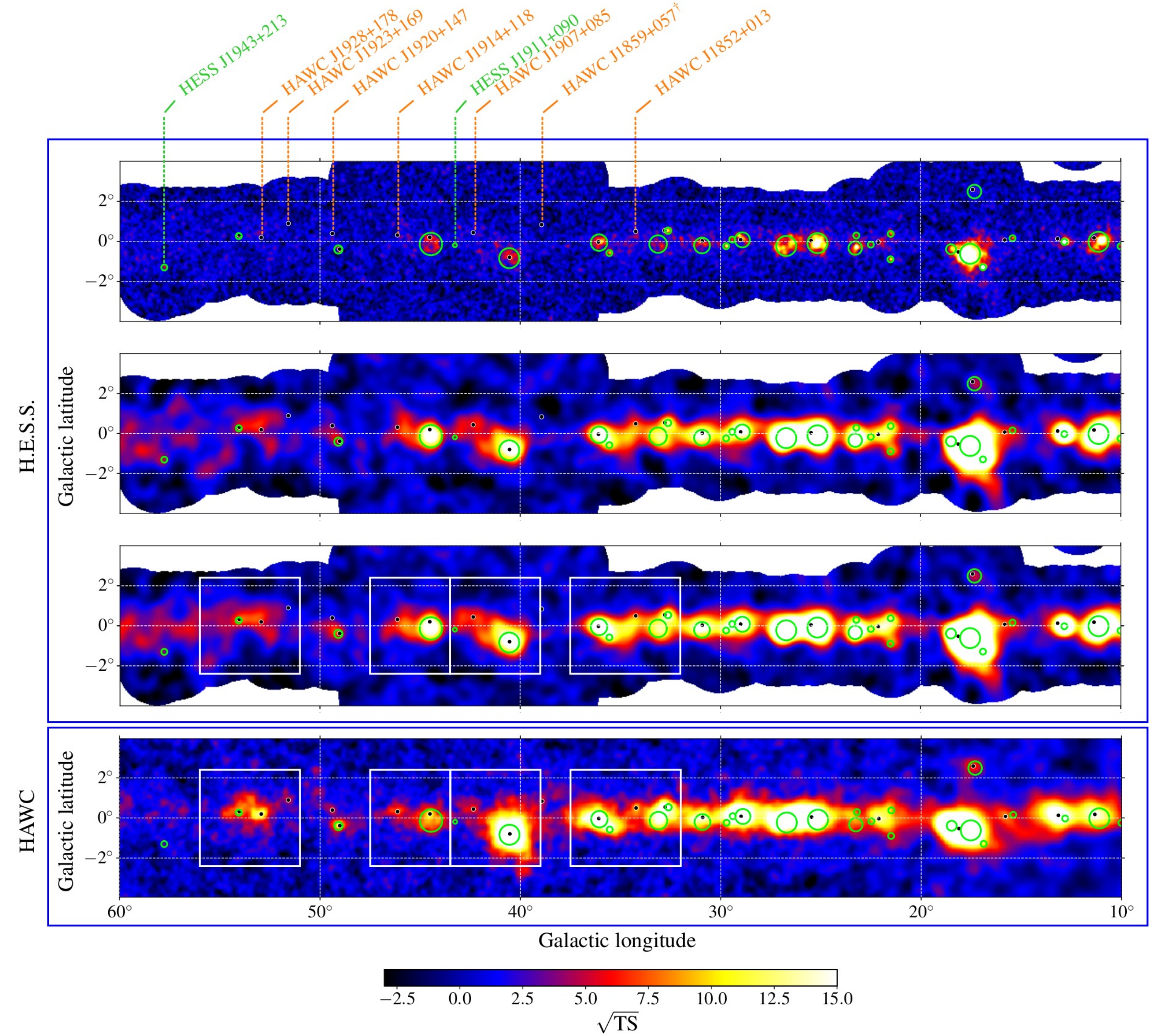

Second HGPS Catalogue – 2HGPS

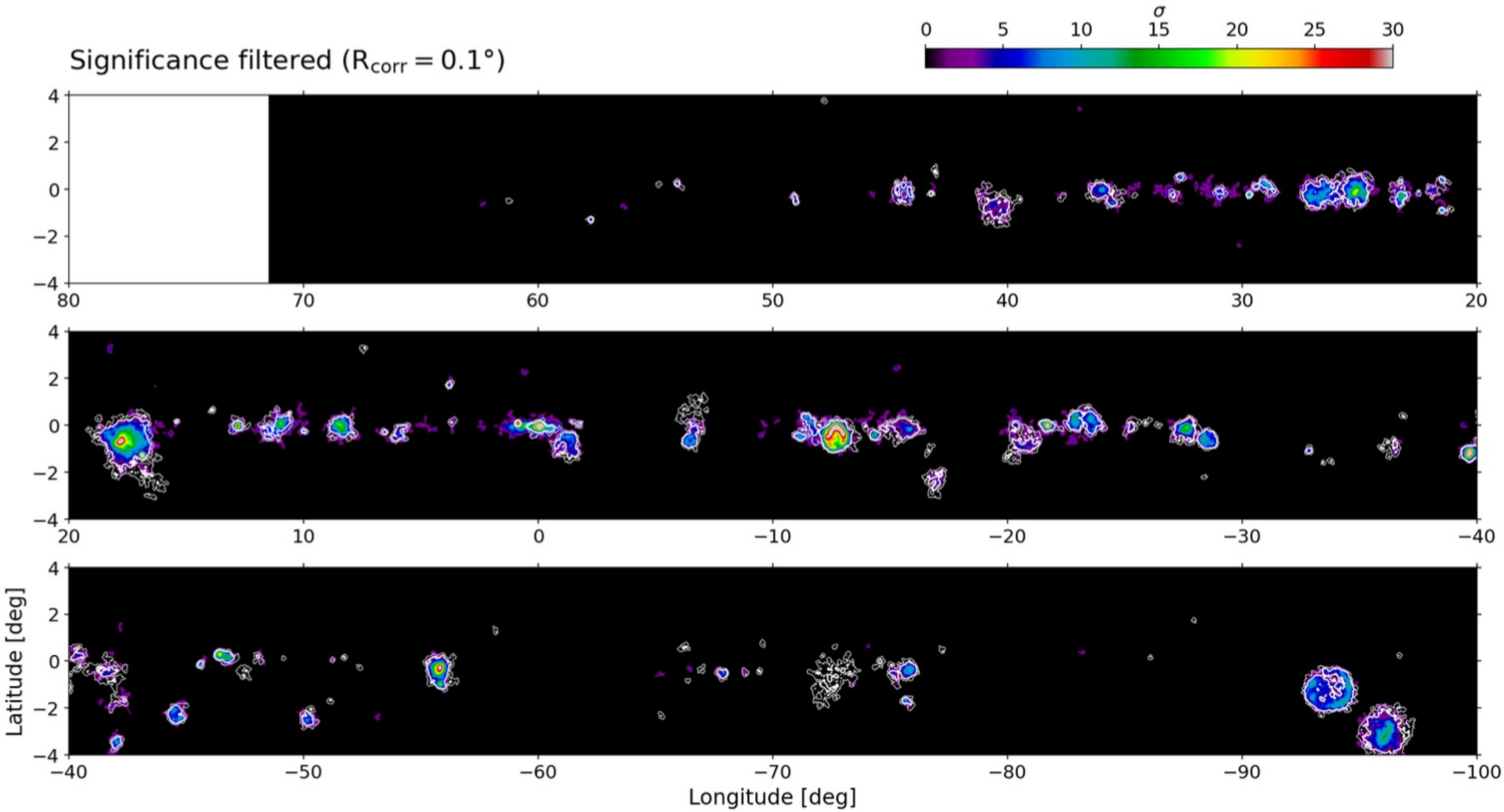

Figure 2: Filtered significance of the excess above the CR background. The map correspond to the result of the HGPS (integrated above 1 TeV) and the contours show the 2HGPS significance at 3 and 8σ (integrated in the 0.5-100 TeV energy range). The spatial bins width is 0.02° for both.

PeVatrons – Galactic centre

*H.E.S.S. Collaboration, Nature **531**, 476 (2016)*

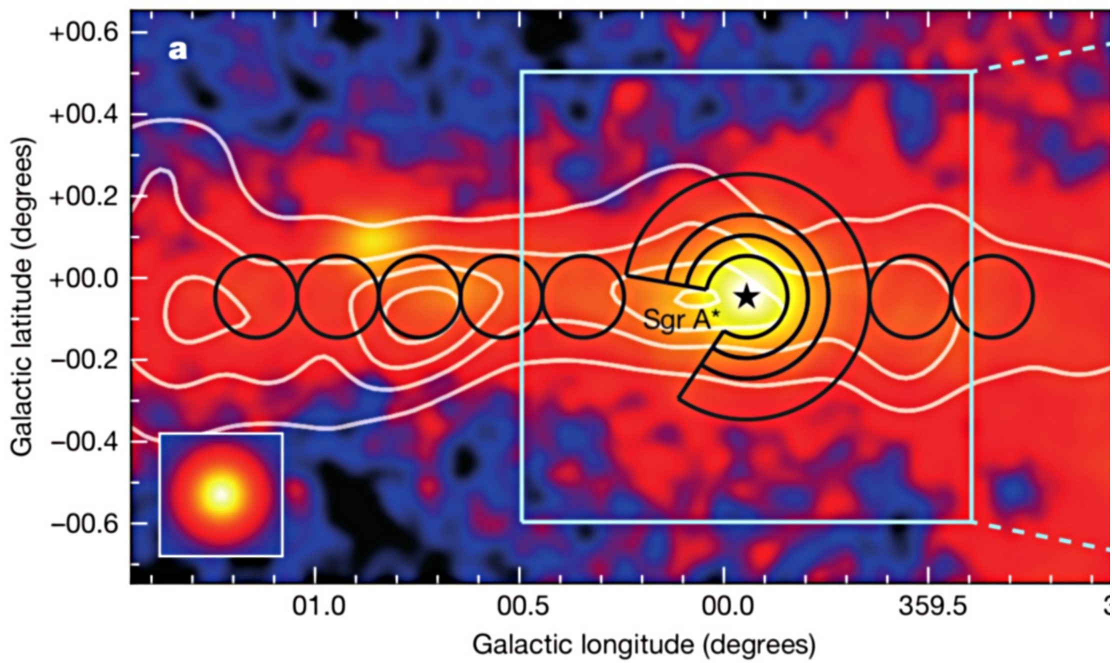

Figure 1 | VHE γ-ray image of the Galactic Centre region. The colour scale indicates counts per 0.02° × 0.02° pixel. **a**, The black lines outline the regions used to calculate the cosmic-ray energy density throughout the central molecular zone. A section of 66° is excluded from the annuli (see Methods). White contour lines indicate the density distribution of

molec
Sgr A
the in
~70 p
diffus

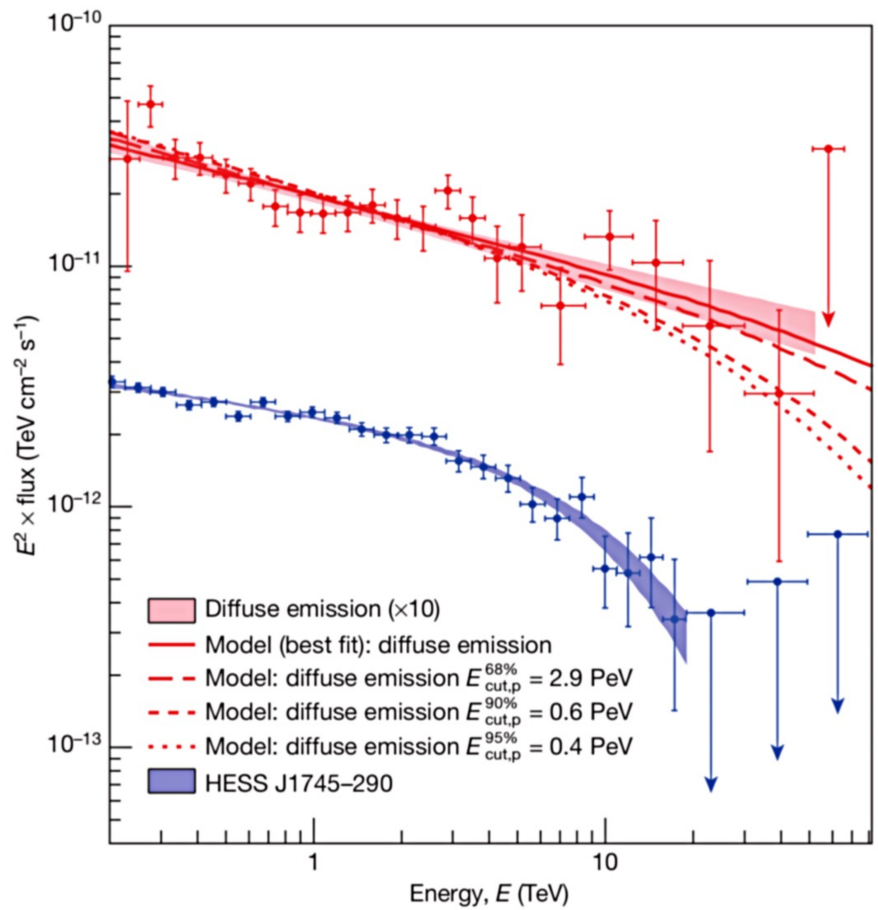

Figure 3 | VHE γ-ray spectra of the diffuse emission and HESS J1745−290. The y axis shows fluxes multiplied by a factor E^2, where E is the energy on the x axis, in units of TeV cm^{-2} s^{-1}. The vertical and horizontal error bars show the 1σ statistical error and the bin size, respectively. Arrows represent 2σ flux upper limits. The 1σ confidence bands of the best-fit spectra of the diffuse and HESS J1745−290 are shown in red and blue shaded areas, respectively. Spectral parameters are given in Methods. The red lines show the numerical computations assuming that γ-rays result from the decay of neutral pions produced by proton–proton interactions. The fluxes of the diffuse emission spectrum and models are multiplied by 10.

– Recent searches for a high-energy cut-off in the spectrum of the diffuse emission around Sgr A∗ have led to unclear conclusions, with MAGIC reporting a 2σ hint for a spectral turnover around ≈ 20 TeV and VERITAS measuring a straight power law up to 40 TeV (MAGIC Collaboration et al. 2020; Adams et al. 2021)

PeVatrons – HESS J1702-420

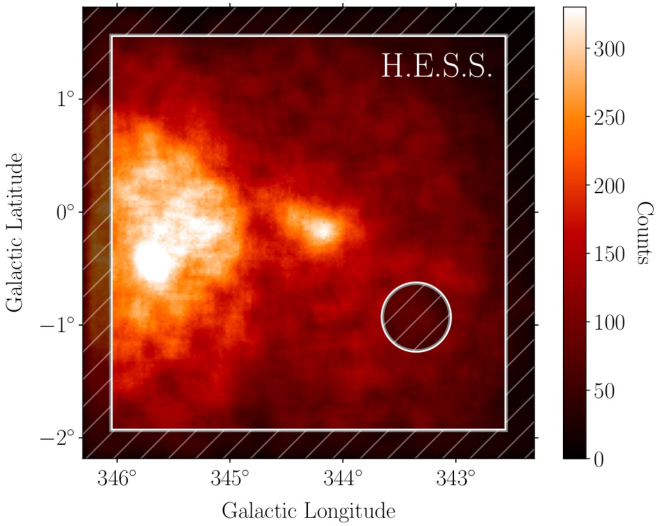

H.E.S.S. Collaboration, A&A (2021)

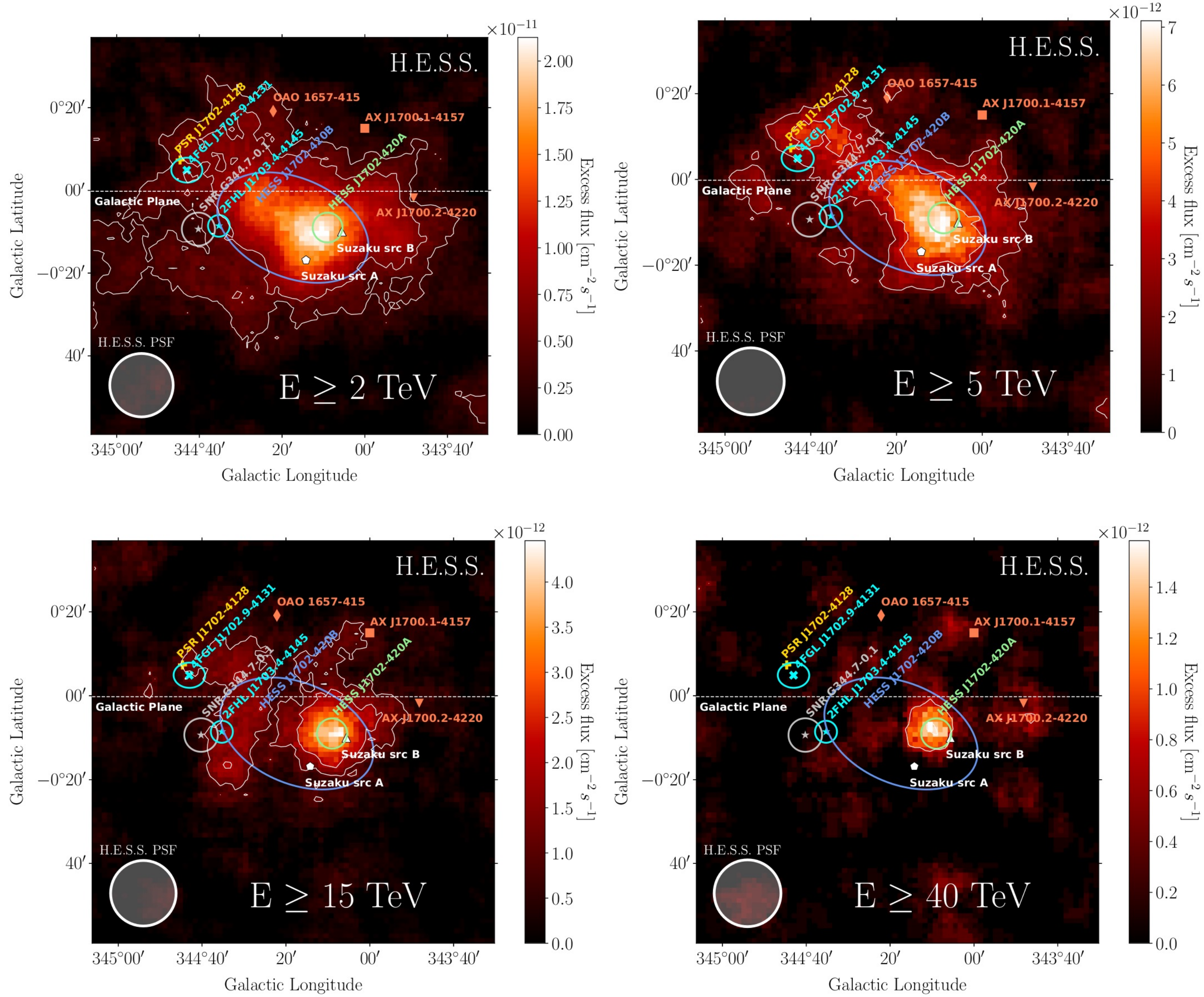

– two separate components – both detected at > 5σ confidence level — inside HESS J1702-420 based on their different morphologies and γ-ray spectra

PeVatrons – HESS J1702-420

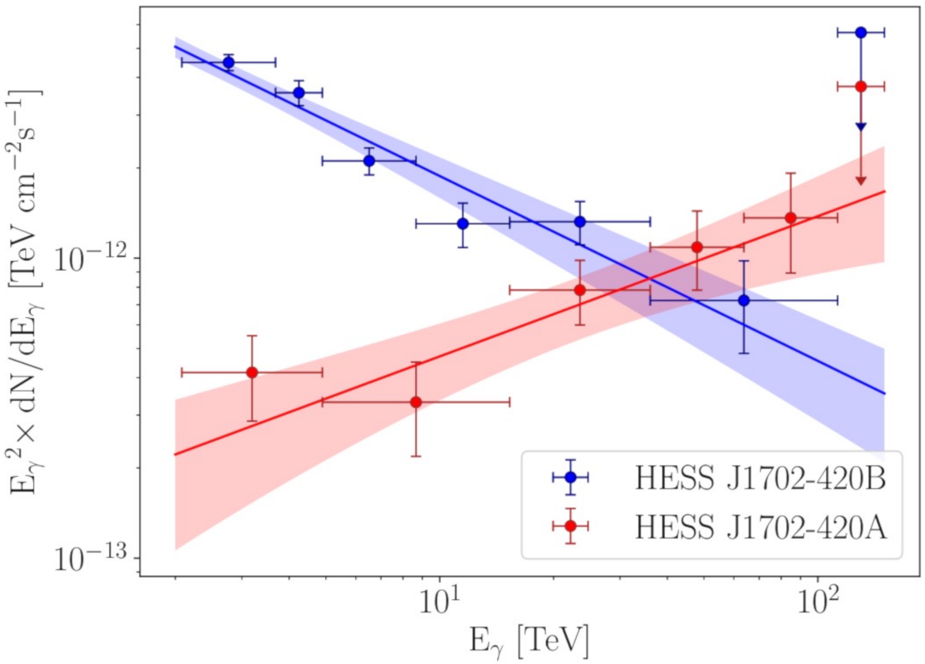

H.E.S.S. Collaboration, A&A (2021)

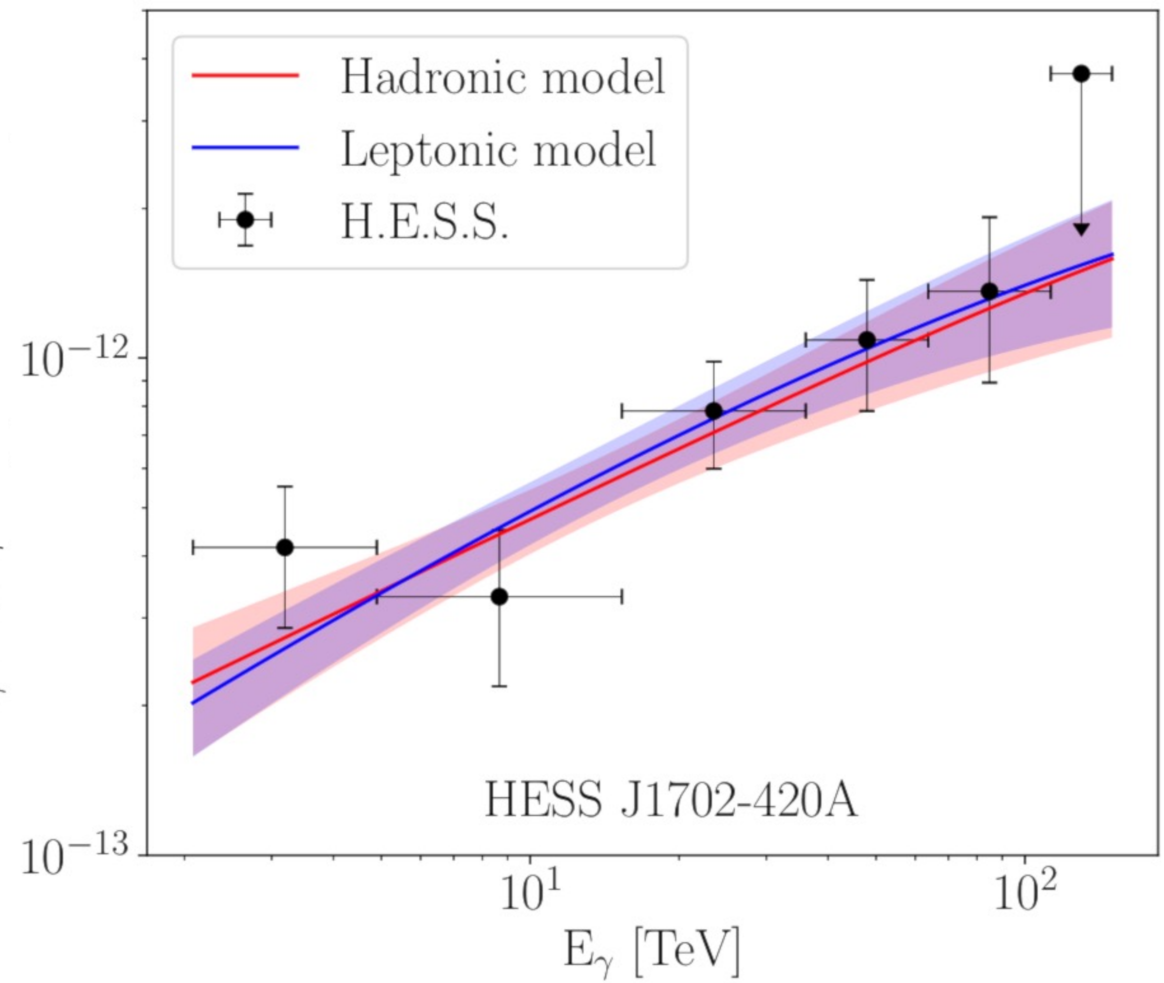

– detection of gamma-ray emission from HESS J1702-420A in the **energy band 64-113 TeV**

The 95% confidence level energy cut-off of the baseline proton (electron) distribution of HESS J1702-420A was found in the range **0.55 – 1.16 PeV** (64 – 152 TeV)

Vela pulsar with CT5 in mono mode

H.E.S.S. Collaboration, A&A (2018)

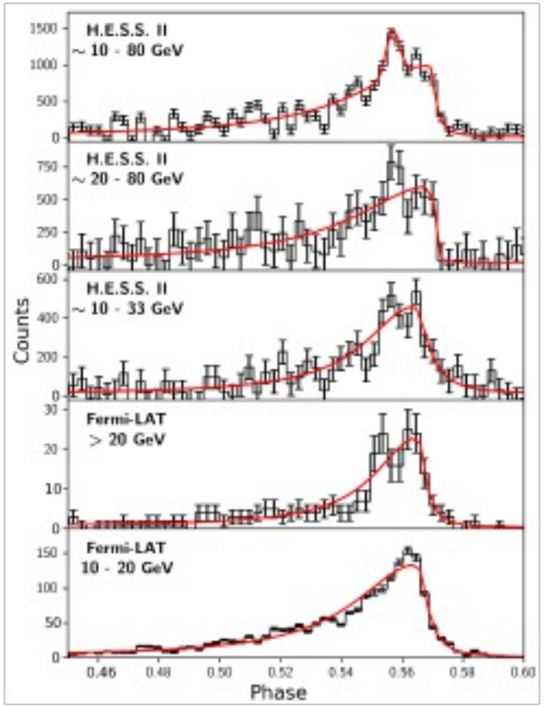

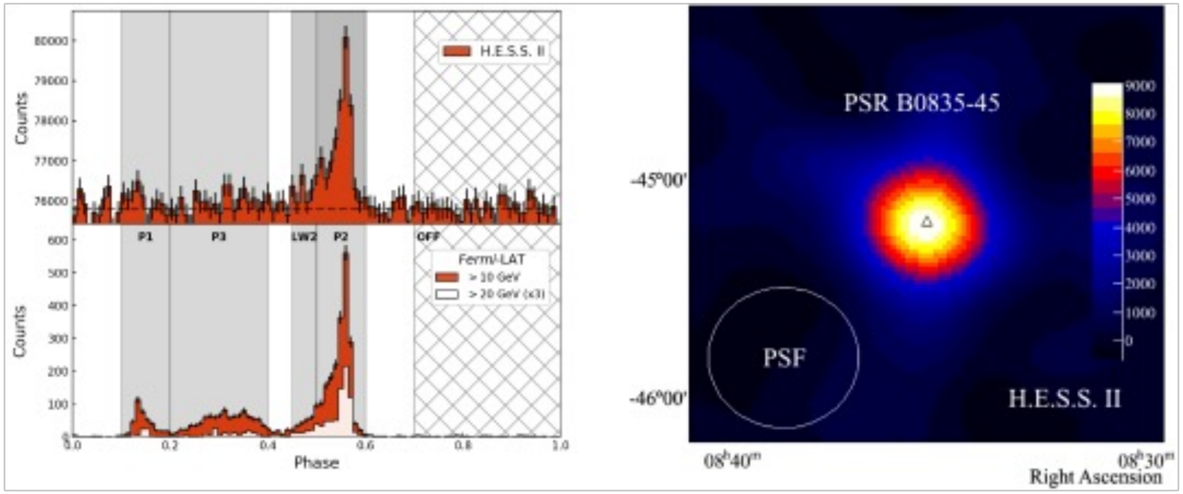

Left: γ-ray phasogram of the Vela pulsar from H.E.S.S. II-CT5 data (top panel) and 96 months of Fermi-LAT data above 10 and 20 GeV (bottom panel). Right: Gaussian-smoothed excess map for the CT5 data in the P2 phase range.

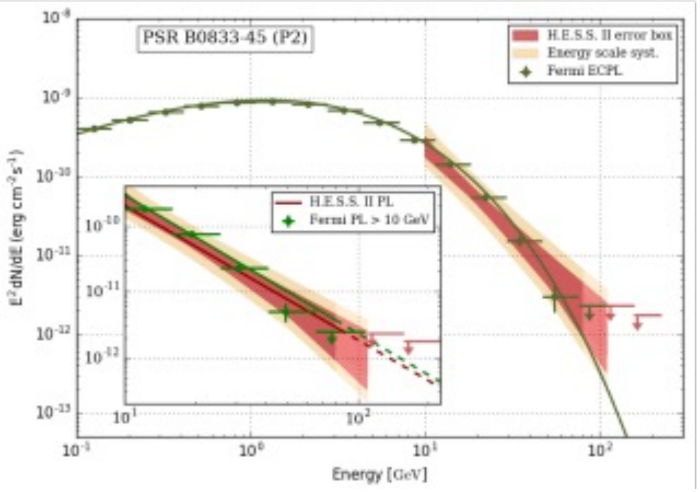

– pulsed high-energy γ-ray emission from the Vela pulsar, PSR B0833−45, based on 40.3 h observations with the largest telescope of H.E.S.S., CT5, in monoscopic mode
– a pulsed γ-ray signal at a significance level of more than 15σ is detected from the P2 peak of the Vela pulsar light curve
– of a total of 15 835 events, more than **6000 lie at an energy below 20 GeV**
– CT5 data show a **change in the pulse morphology of P2**, i.e. an extreme sharpening of its trailing edge, together with the **possible onset of a new component** at 3.4σ significance level

Vela pulsar with H.E.S.S.

H.E.S.S. Collaboration (2023).

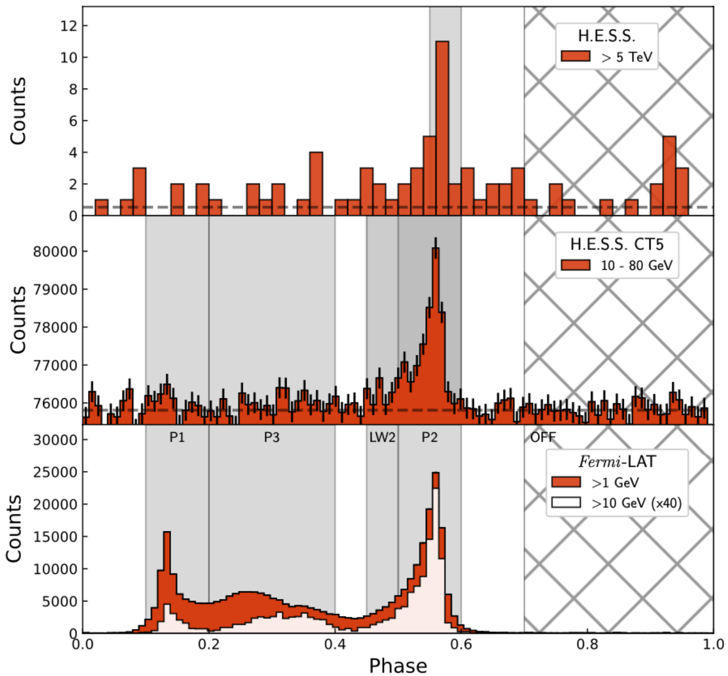

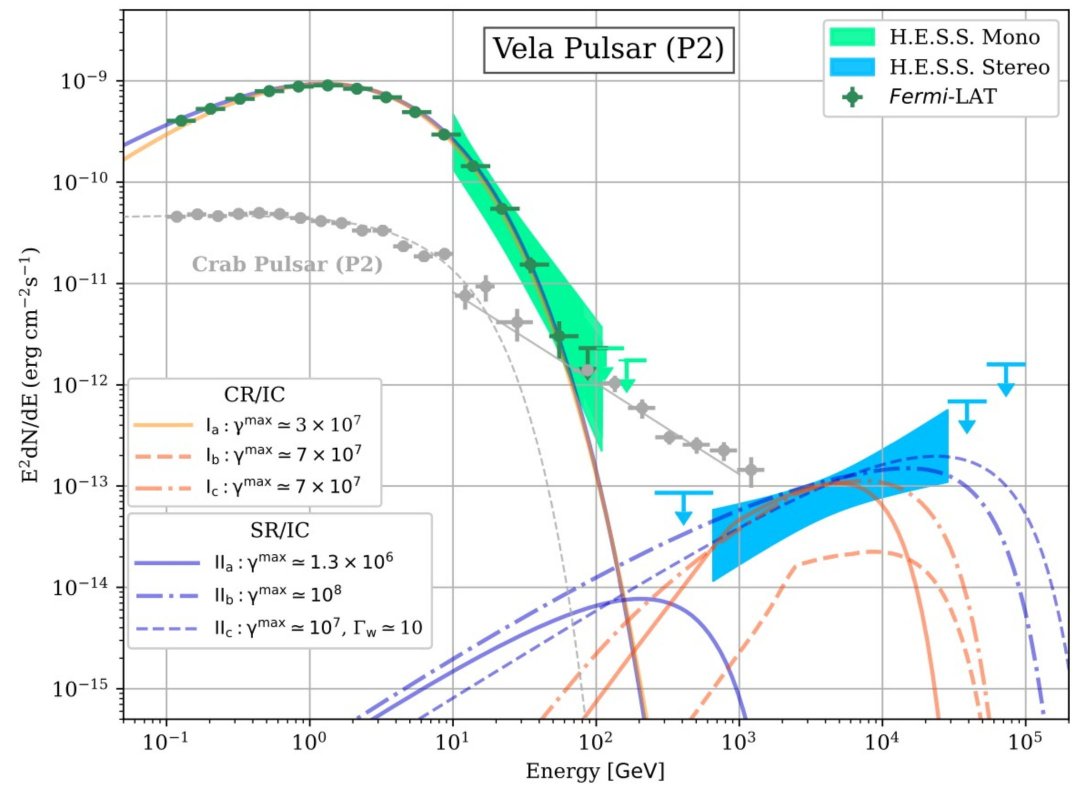

Fig. 3 Spectral energy distribution (SED) of the P2 pulse of Vela

Our discovery opens a new observation window for detection of other pulsars in the TeV to the tens of TeV range with current and upcoming more sensitive instruments.

Vela pulsar with H.E.S.S.

H.E.S.S. Collaboration (2023).

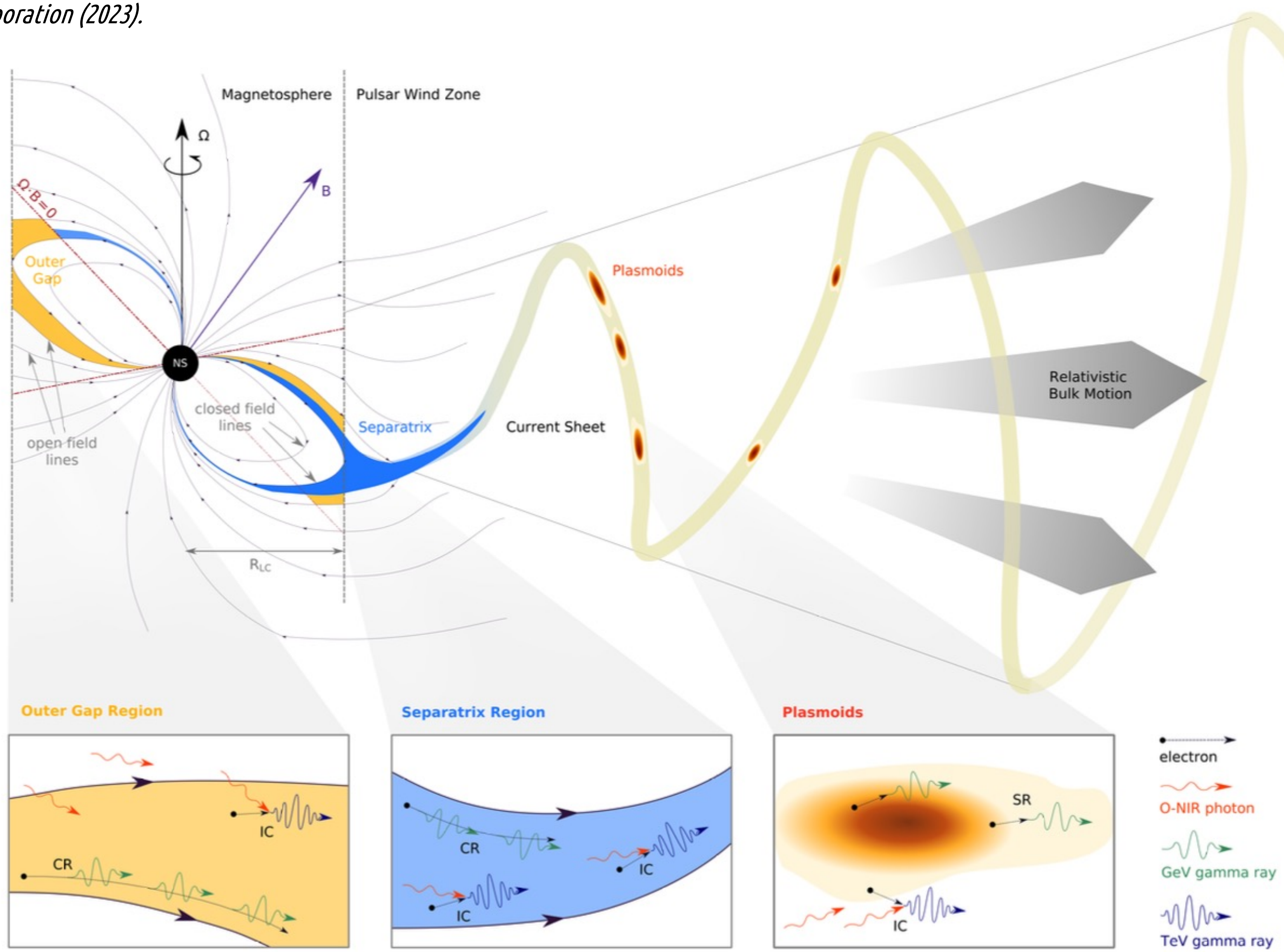

SS433 with H.E.S.S.

SS 433 (V1343 Aql) is a binary system comprising a compact object, likely a black hole, and a type A supergiant star

H.E.S.S. Collaboration (2024).

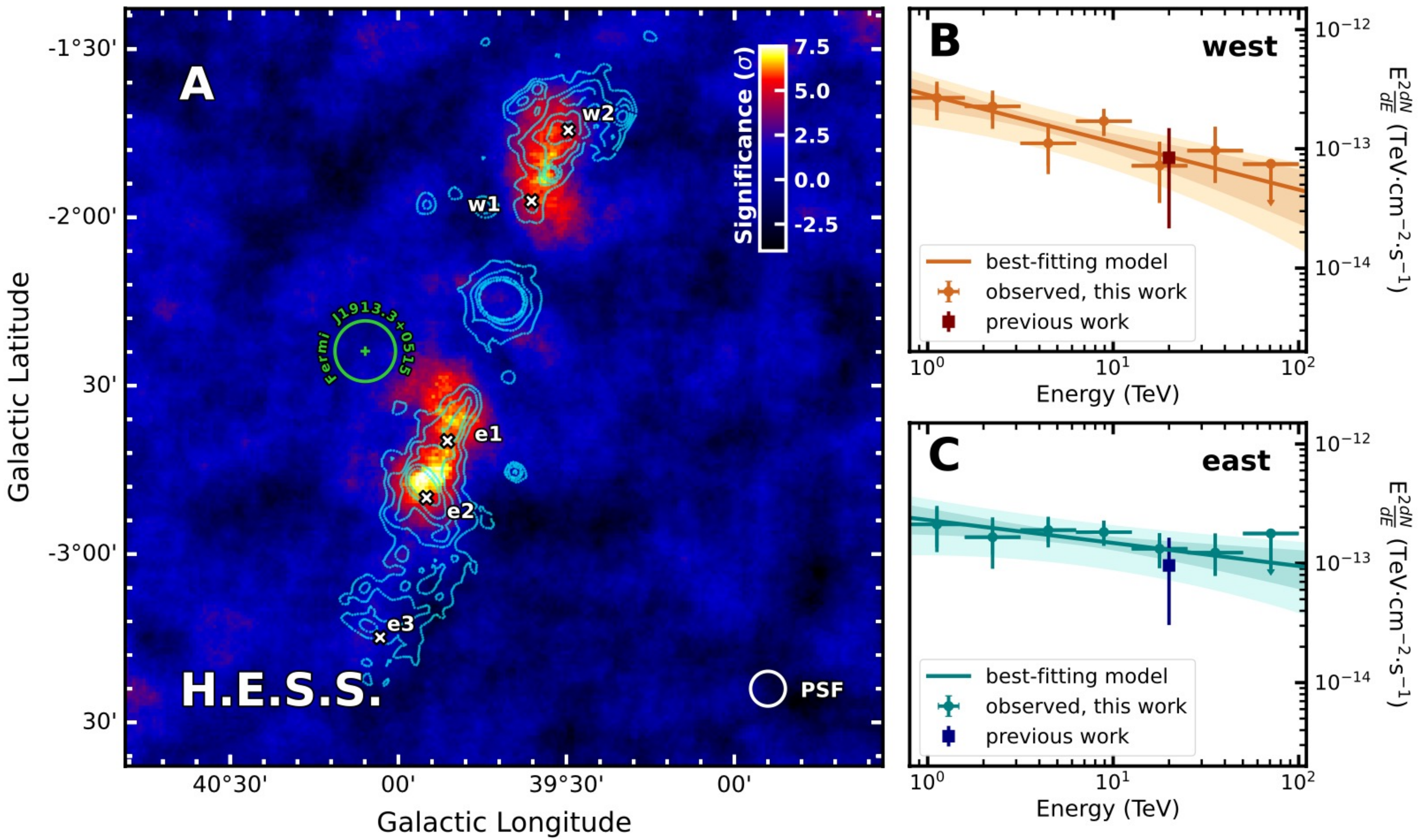

SS433 with H.E.S.S.

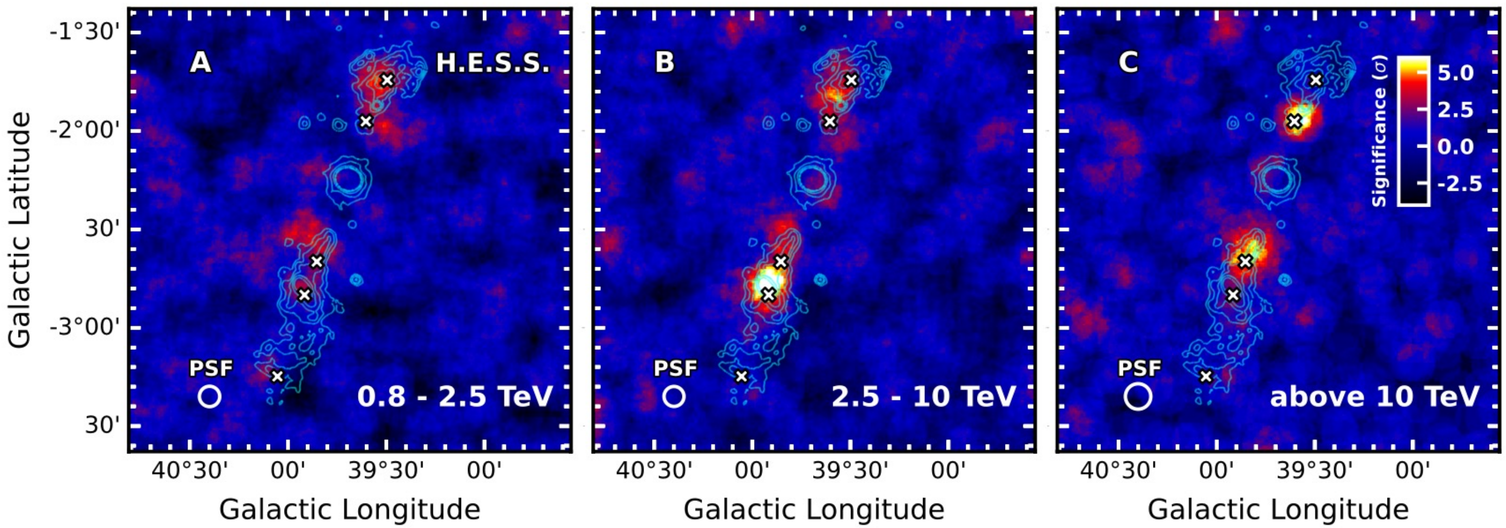

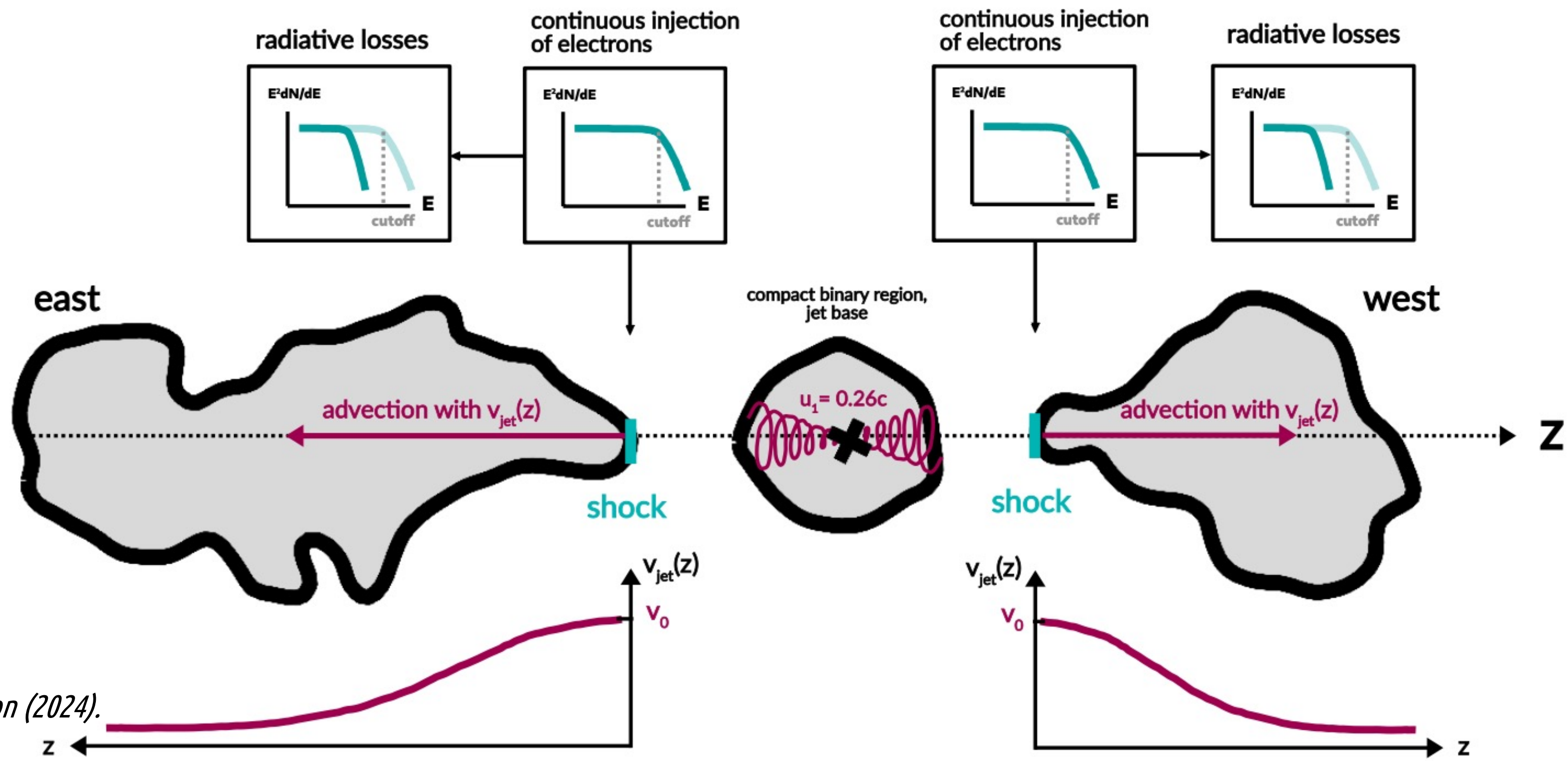

H.E.S.S. Collaboration (2024).

Multi-wavelength campaign on M87

*EHT Collaboration et al., ApJL **911**, L11 (2021)*

– the most extensive, quasi-simultaneous, broad- band observations of M87 taken yet, together with the highest ever resolution mm-VLBI images

– substantial contribution of all VHE observatories

– the M87 core was in a relatively low state compared to historical observations, but clearly still dominating over the nearest knot HST-1, which was seemingly at its lowest historical brightness state

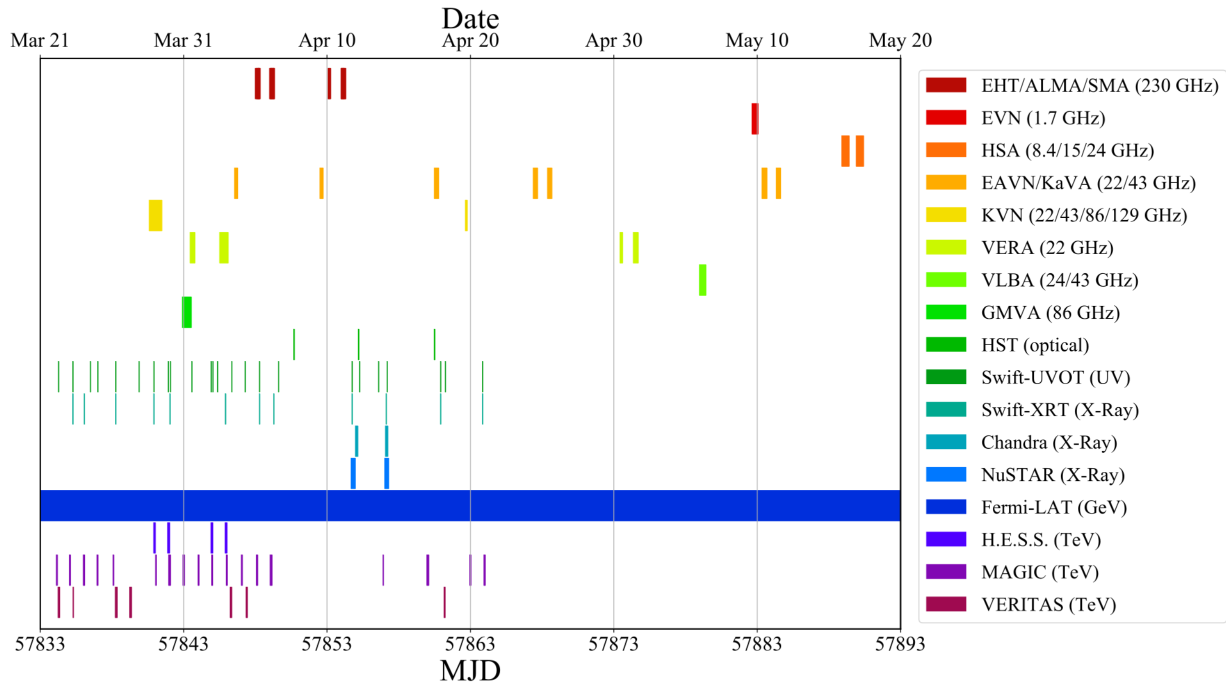

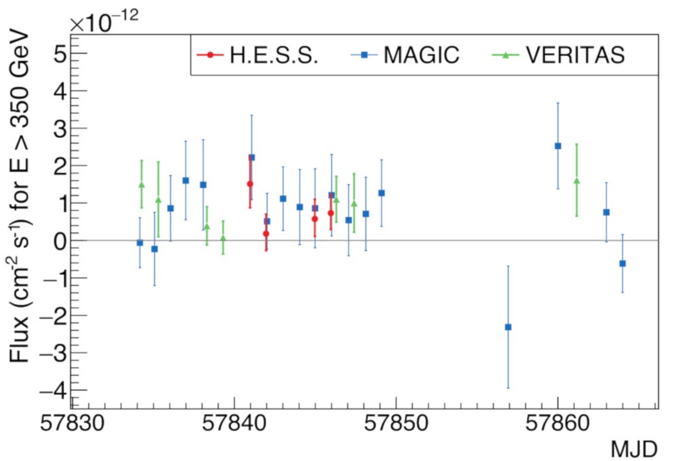

Figure 11. Flux measurements of M87 above 350 GeV with 1σ uncertainties obtained with H.E.S.S., MAGIC, and VERITAS during the coordinated MWL campaign in 2017. Upper limits for flux points with a significance below 2σ are provided in Table A7 in Appendix A.

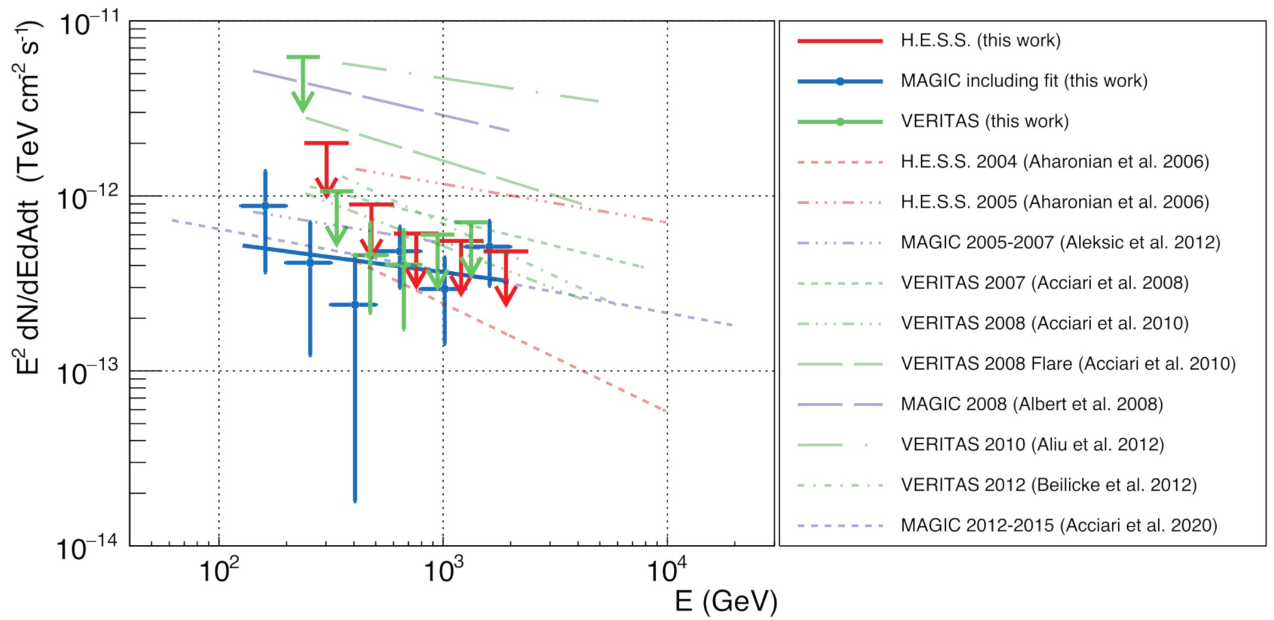

Multi-wavelength campaign on M87

*EHT Collaboration et al., ApJL **911**, L11 (2021)*

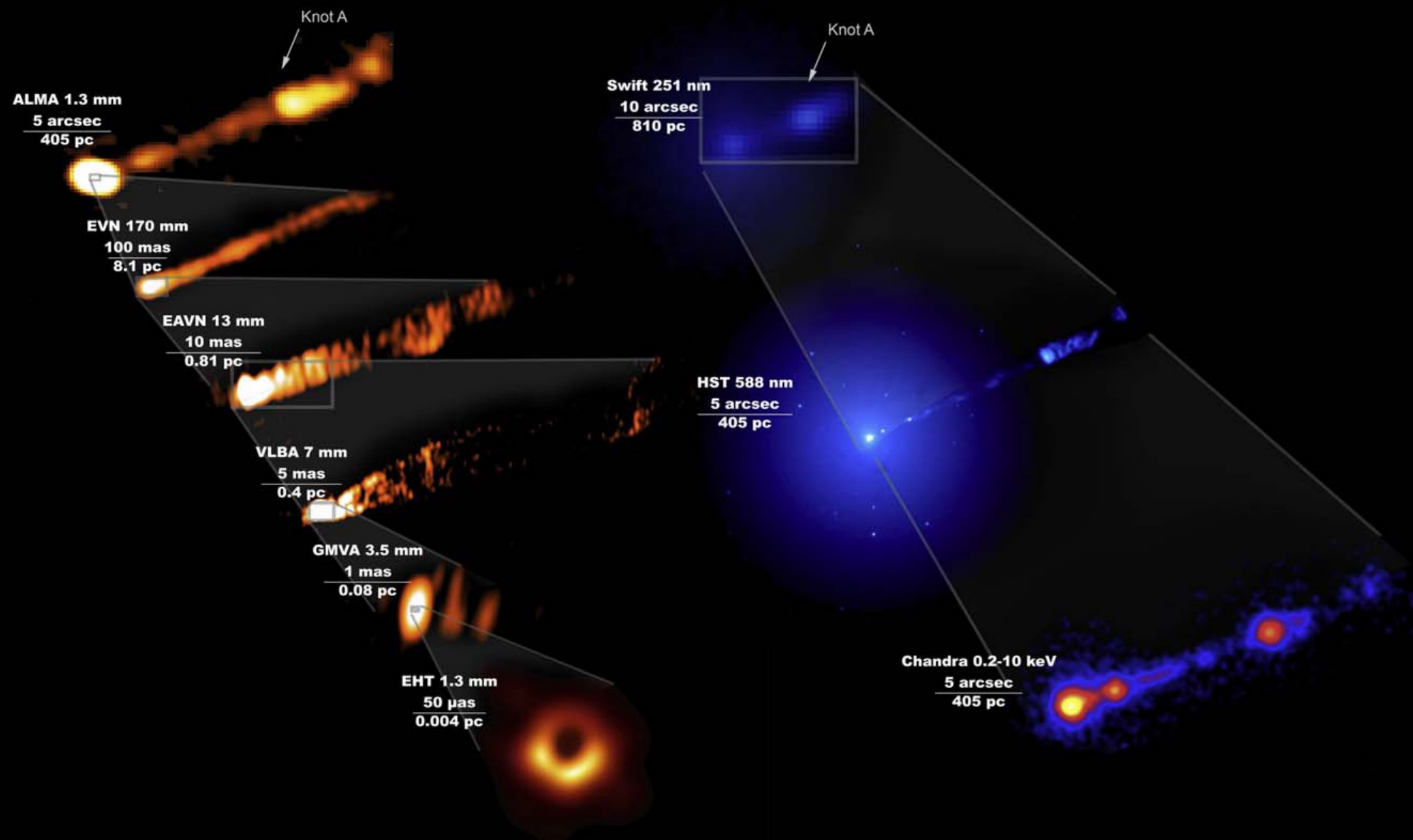

Multi-wavelength campaign on M87

EHT Collaboration et al., ApJL ***911****, L11 (2021)*

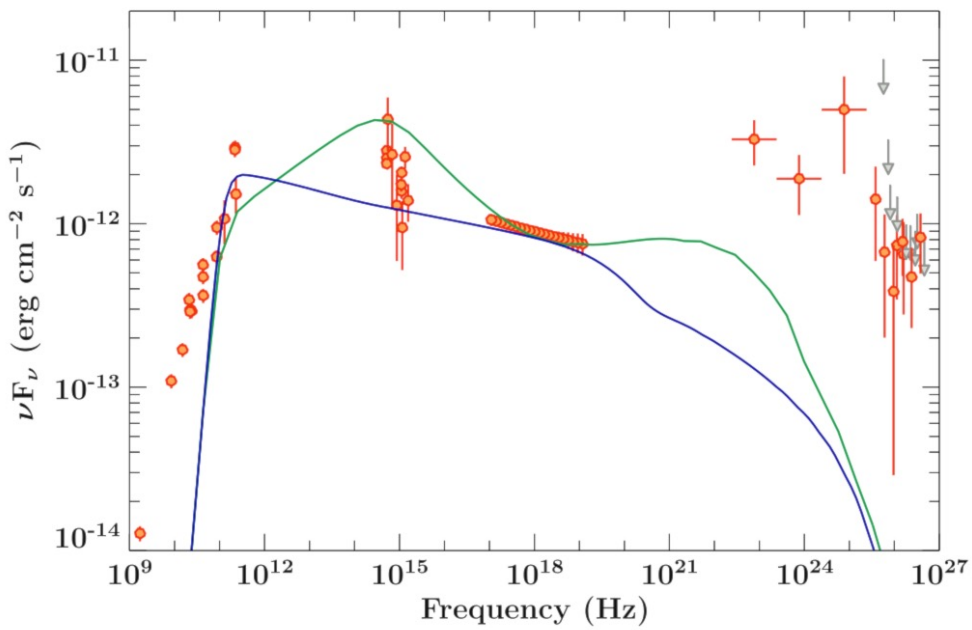

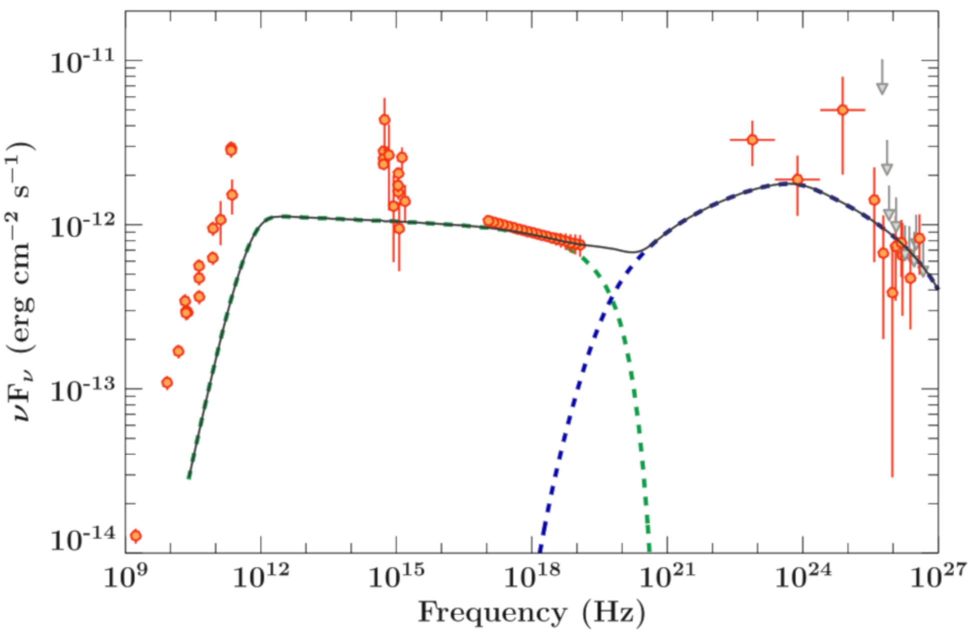

– nor a single-zone model that aims to provide a straightforward description of the flux and compact emission region size measured by EHT and other VLBI facilities (with or without radiative cooling) nor fit to the HE data provides satisfactory explanation of the overall emission

– M87's complex, broadband spectral energy distribution cannot be modeled by a single zone

– it is not yet clear where the VHE γ-rays originate, but it can be robustly rule out that they coincide with the EHT region for leptonic processes; direct proton and muon synchrotron emission from the EHT-emission region contributing to the GeV/TeV range cannot be ruled out

LMC P3 – γ-ray binary in the Large Magellanic Cloud

– past observations led to the discovery of three individual very-high-energy γ-ray-emitting sources in LMC (H.E.S.S. Collaboration 2015): superbubble 30 Dor C, pulsar wind nebula PWN N157B, core-collapse supernova remnant SNR N132D.

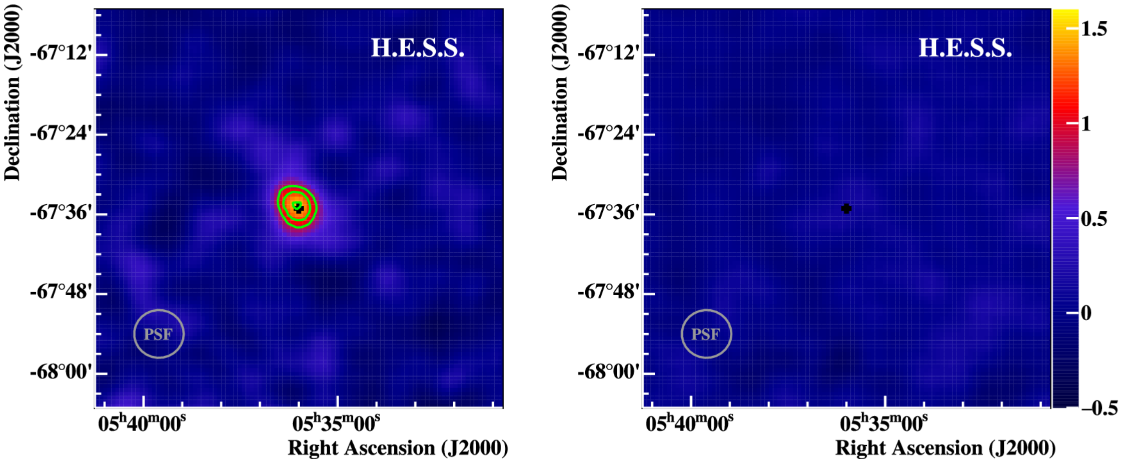

H.E.S.S. excess count rate maps for the on-peak (left panel) and off-peak (right panel) regions of the orbit.

the high-energy γ-ray emission from the object LMC P3 in the Large Magellanic Cloud (LMC) has been discovered to be modulated with a 10.3-day period, making it **the first extra-galactic γ-ray binary**

– LMC P3 is the most luminous γ-ray binary known so far

*HESS Collaboration, A&A **610**, L17 (2018)*

– two scenarios proposed for γ-ray binaries are that the γ-ray emission can be powered either by the **spin-down of a pulsar** or by **accretion of the stellar wind onto the compact object**

– **VHE emission is out of phase with the HE** emission which may be explained by **absorption due to pair production**, or by **different particle distributions** responsible for the HE and VHE γ-ray production

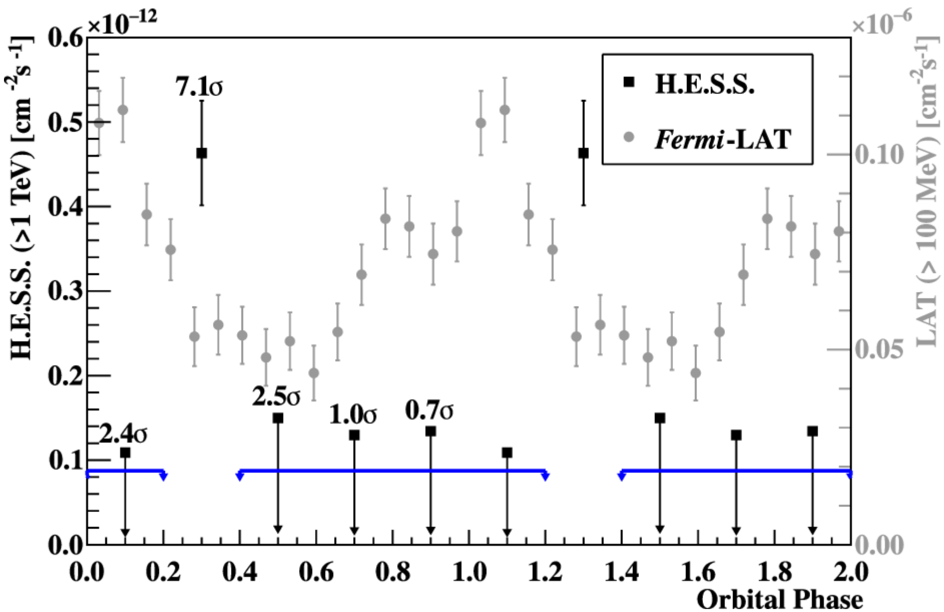

Folded γ-ray light curves with orbital phase zero at the maximum of the HE γ-ray emission (MJD 57 410.25)

LMC P3 – γ-ray binary in the Large Magellanic Cloud

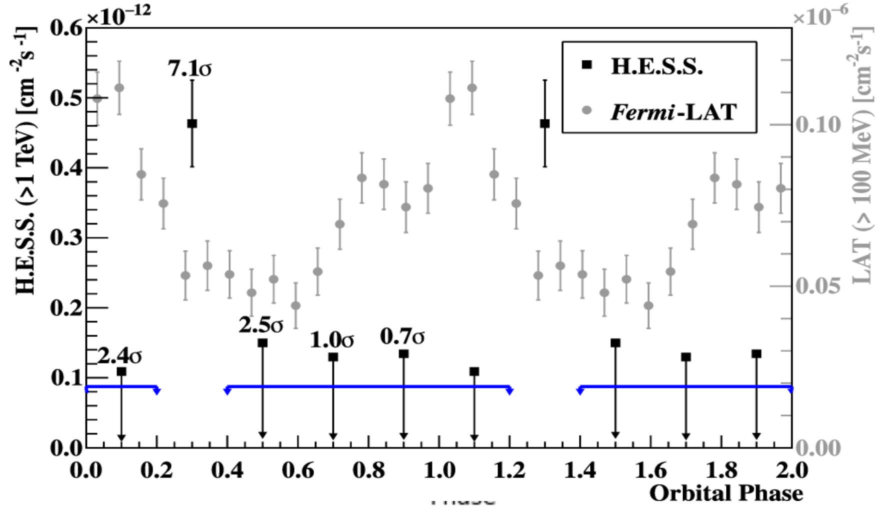

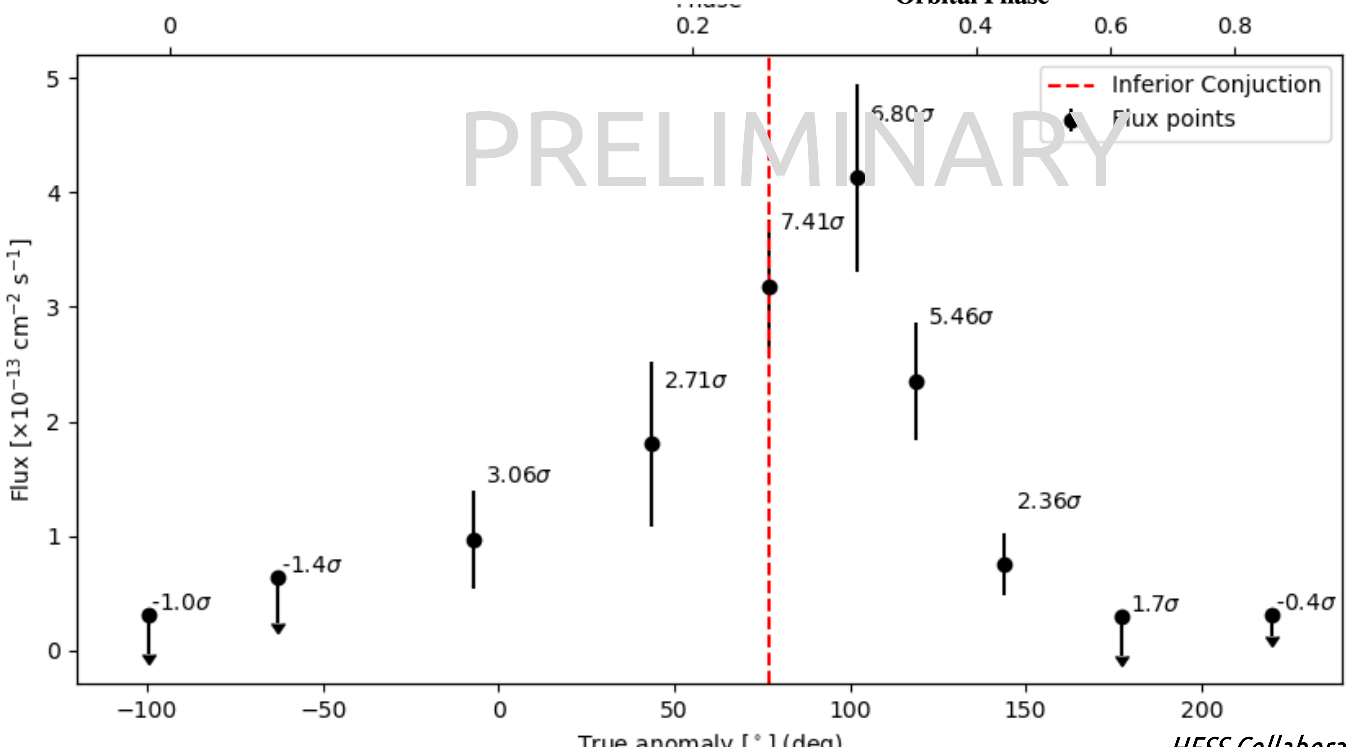

HESS Collaboration , ICRC2023 (2024)

LMC N132D – γ-ray SNR in the Large Magellanic Cloud

HESS Collaboration, A&A (2021)

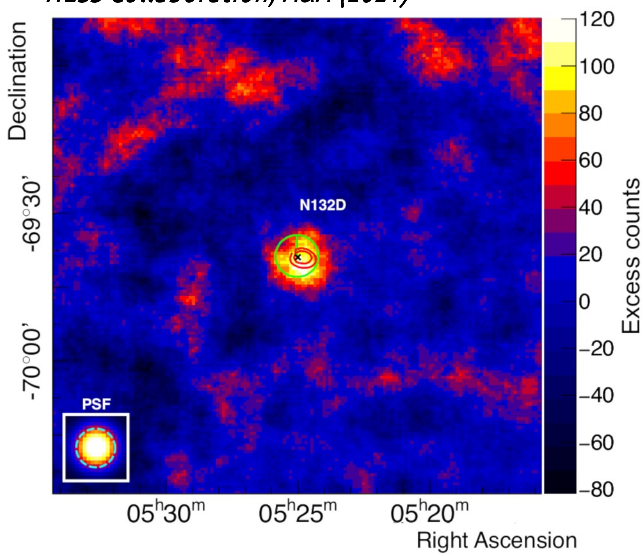

– The LMC SNR N132D is detected with a statistical significance of 5.7 σ above 1.3 TeV

– The Fermi-LAT and H.E.S.S. gamma-ray spectrum extends up to 15 TeV and is well described with a power-law index of 2.13 ± 0.05. No cutoff in energy is needed to explain the spectrum

– **N132D is the only extragalactic SNR detected in gamma rays so far**, and its luminosity is compatible with that of the most luminous Galactic SNR G338.3-0.0

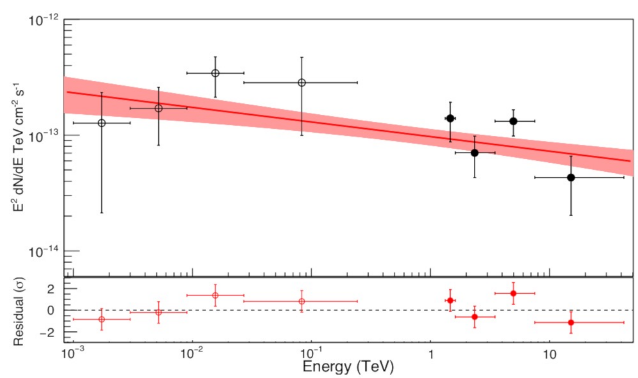

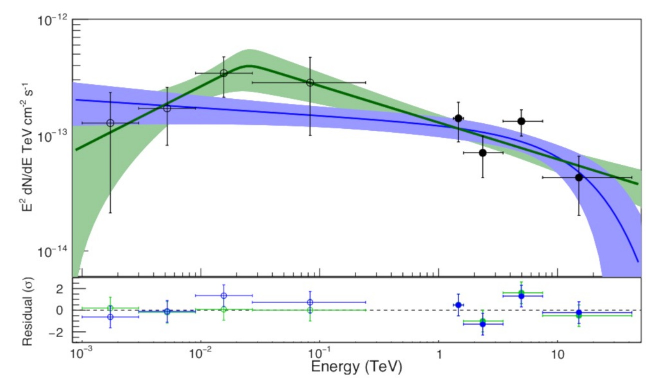

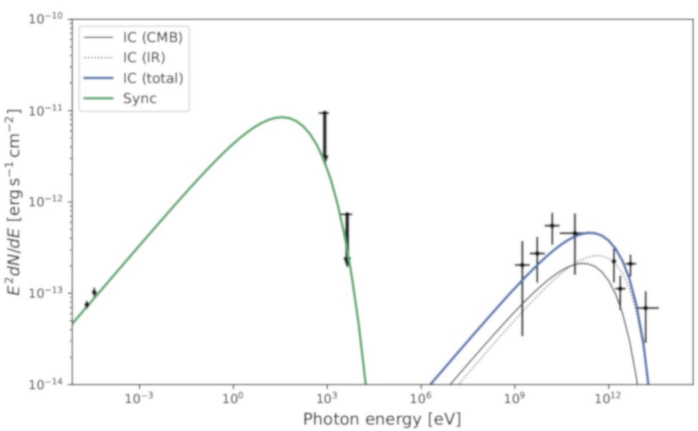

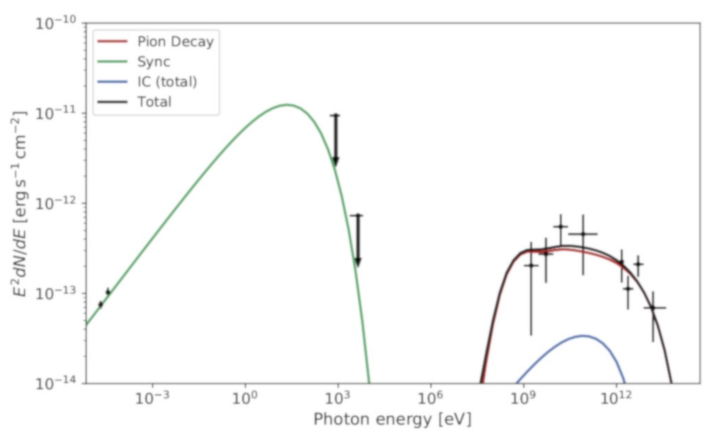

– A purely leptonic model fails to satisfactorily explain the multiwavelength spectrum of N132D (total energy of electrons is too high, the magnetic field strength surprisingly low)

GRBs at VHE

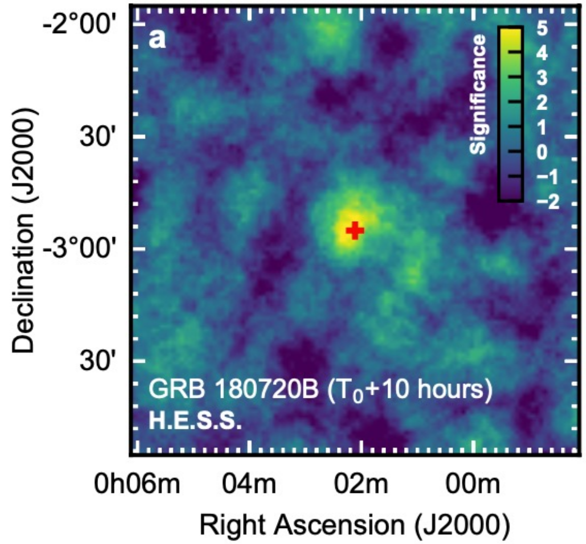

– Three GRBs detected so far at VHE: **GRB180720B** (H.E.S.S. Collaboration, 2019, A very-high-energy component deep in the γ-ray burst afterglow, Nature, 575, 464), **GRB190114C** (MAGIC collaboration, 2019, Teraelectronvolt emission from the γ-ray burst GRB 190114C, Nature, 575, 455), **GRB190829A** (H.E.S.S. Collaboration, 2021, Revealing x-ray and gamma ray temporal and spectral similarities in the GRB 190829A afterglow, Science, 372, 1081)

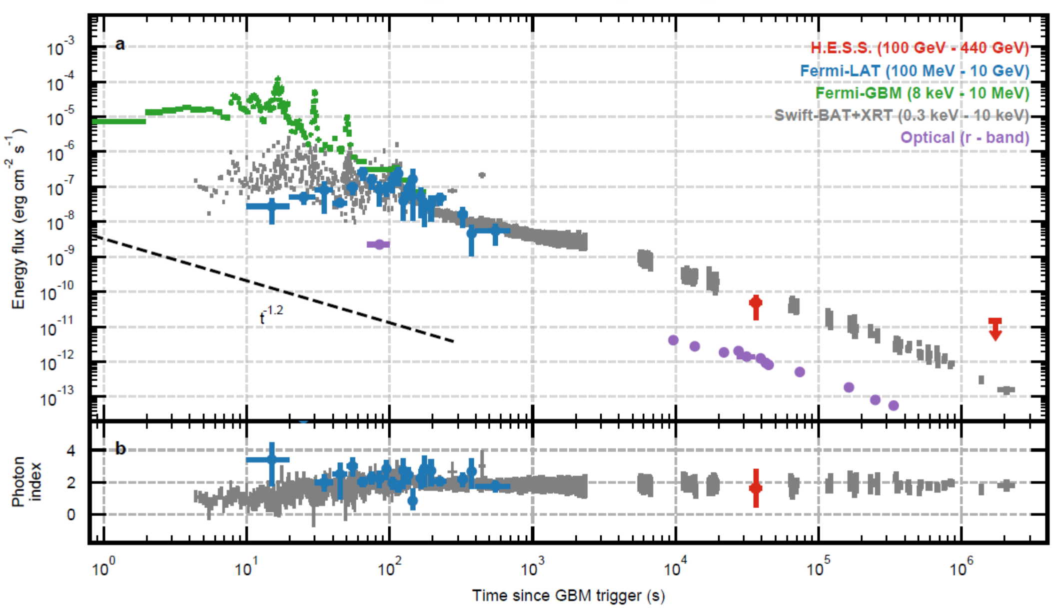

*MAGIC Collaboration, Nature **575**, 459–463 (2019)*

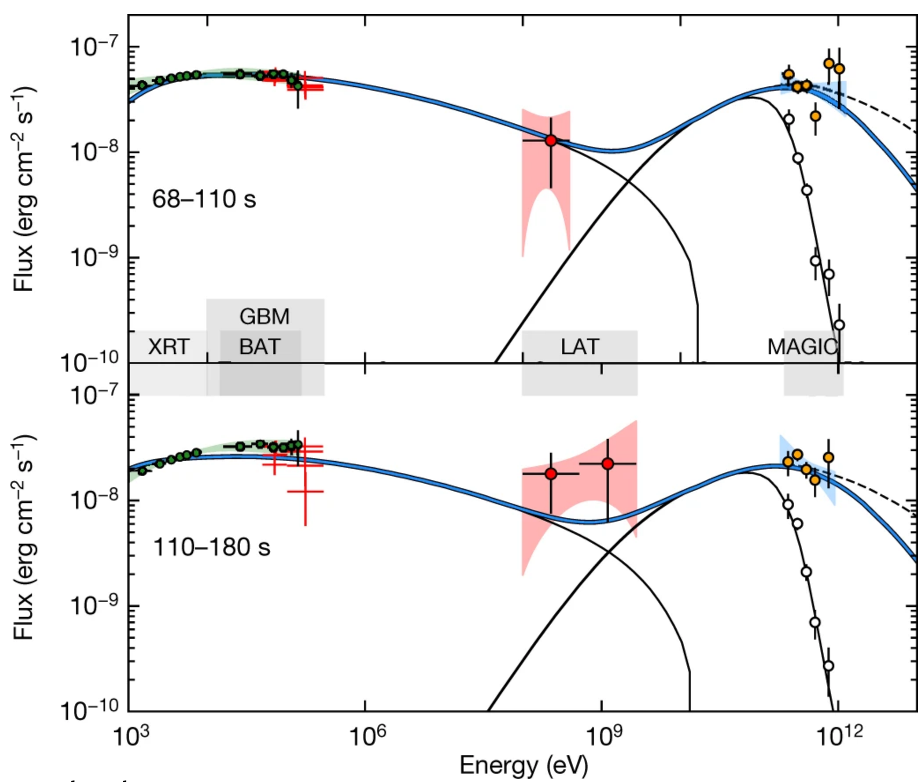

– VHE part of the spectrum usually interpreted as a synchrotron self-Compton (SSC) emission

GRBs at VHE

*H.E.S.S. Collaboration, Science **372**, 1081 (2021)*

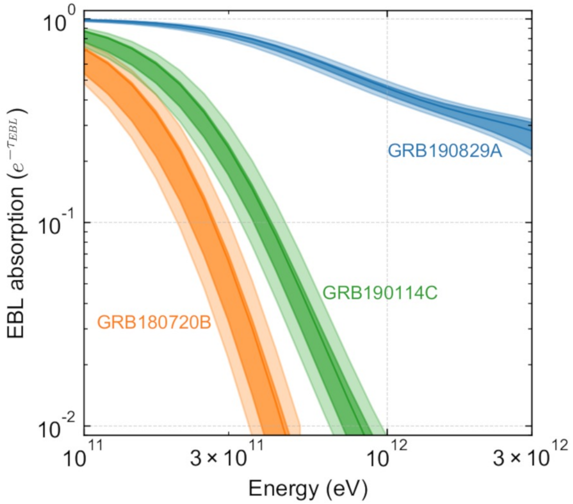

– **GRB190829A** (z=0.0785) observed in three consecutive nights 4h after the prompt emission (21.7 σ in 0.18-3.3 TeV; 5.5 σ in 0.18-1.5 TeV; no detection)
– similarities between the X-ray and VHE gamma-ray emission

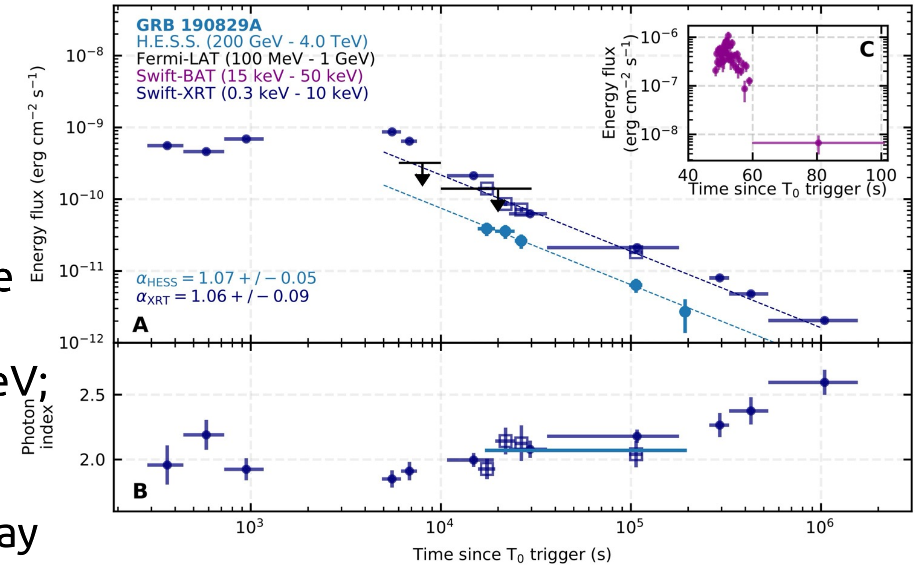

-- no emission from 221009A – the brightest GRB so far (but 53 days after the alert)

-- challenge to SSC interpretation of the VHE emission

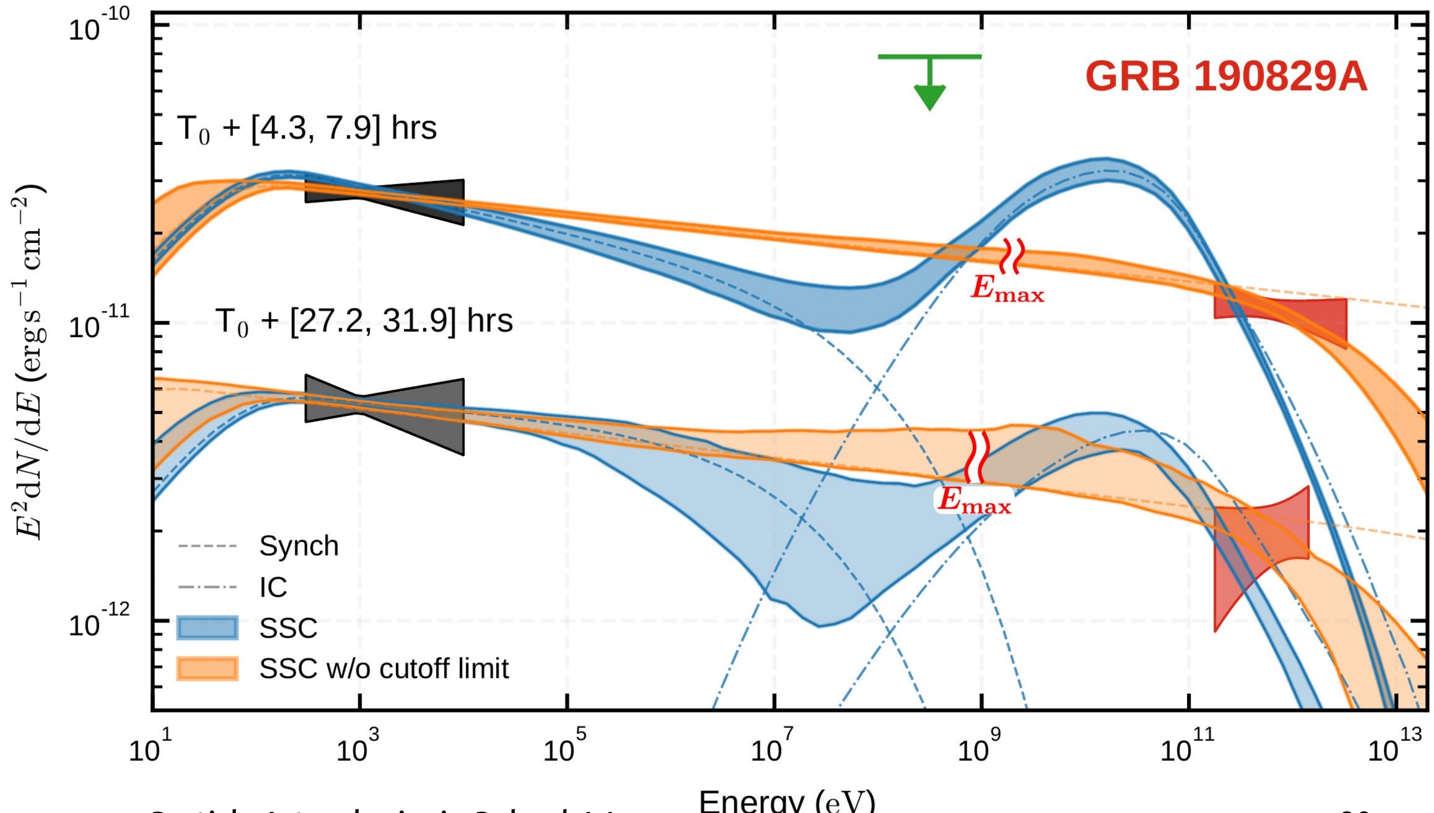

Cosmic-ray electrons with H.E.S.S.

Aharonian et al. (H.E.S.S. Collaboration) (2008).

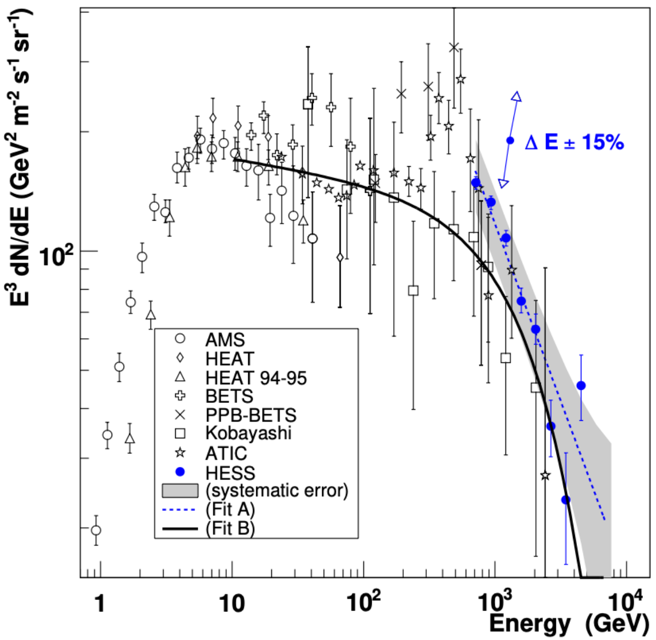

FIG. 3: The energy spectrum E^3 dN/dE of CR electrons as measured by H.E.S.S. in comparison with previous measure-

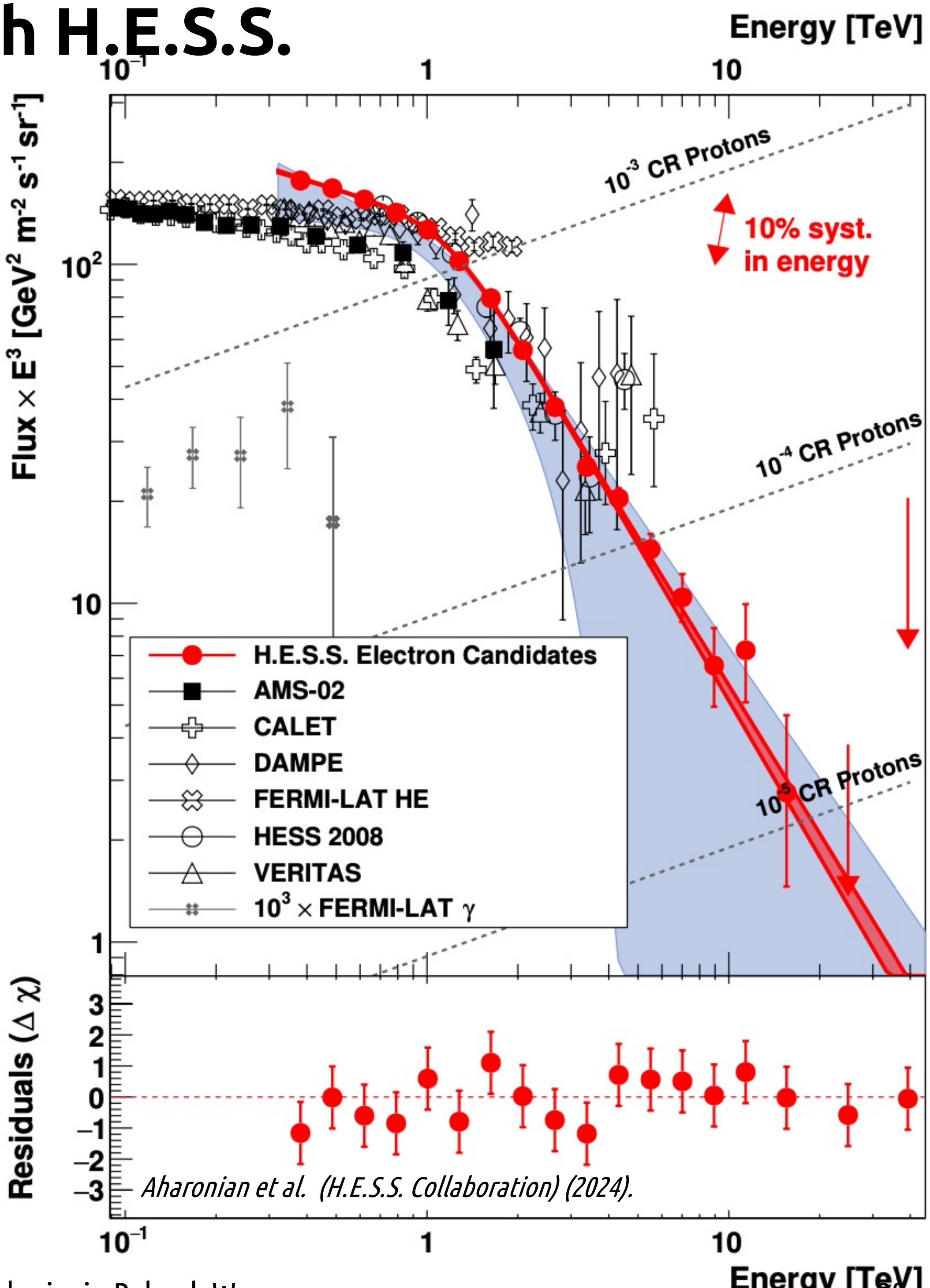

The observed sharp break may therefore favor a scenario in which – at energies around one TeV – **a single nearby source, with a burst-like release of electrons**, takes over a population of CRe escaping from distributed sources

Multi-messenger observations – IceCube-170922A

IceCube Collaboration et al. , Science ***361****, eaat1378 (2018)*

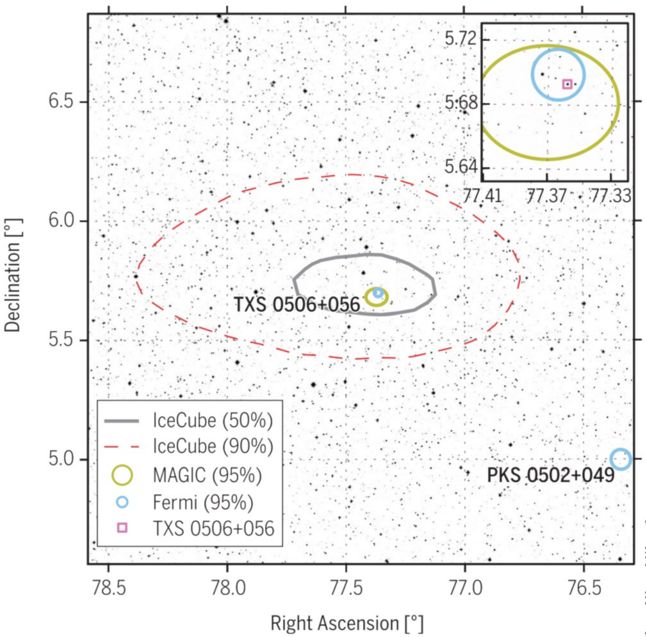

"On 22 September 2017, the cubic-kilometer IceCube Neutrino Observatory detected a ~290-TeV neutrino from a direction consistent with the flaring gamma-ray blazar TXS 0506+056."

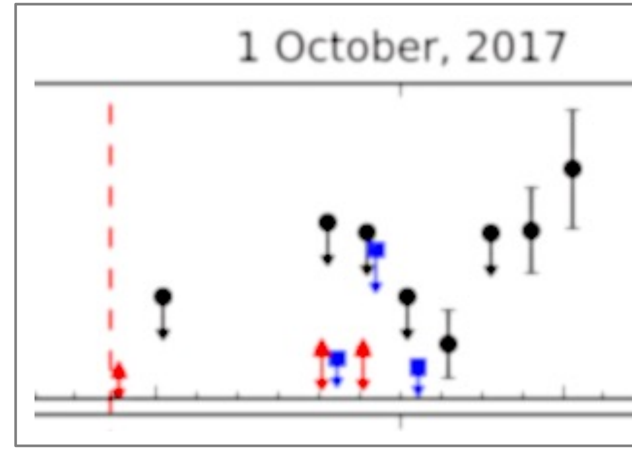

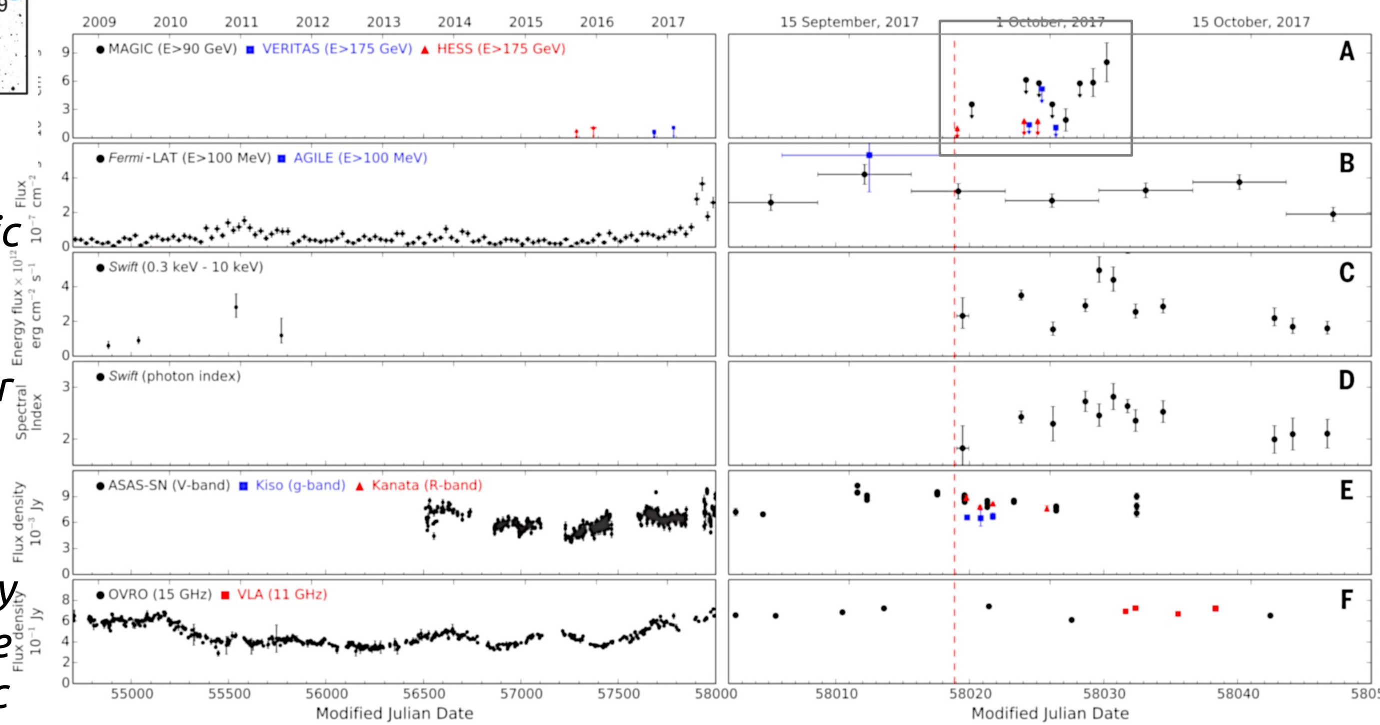

– blazar jets may accelerate cosmic rays to at least several PeV
– the observed association of a high-energy neutrino with a blazar during a period of enhanced g-ray emission suggests that blazars may indeed be one of the long-sought sources of very-high-energy cosmic rays, and hence responsible for a sizable fraction of the cosmic neutrino flux observed by IceCube

Multi-messenger observations – neutrinos

FACT, Fermi-LAT, H.E.S.S., IceCube, MAGIC and VERITAS collaborations, ICRC 2023

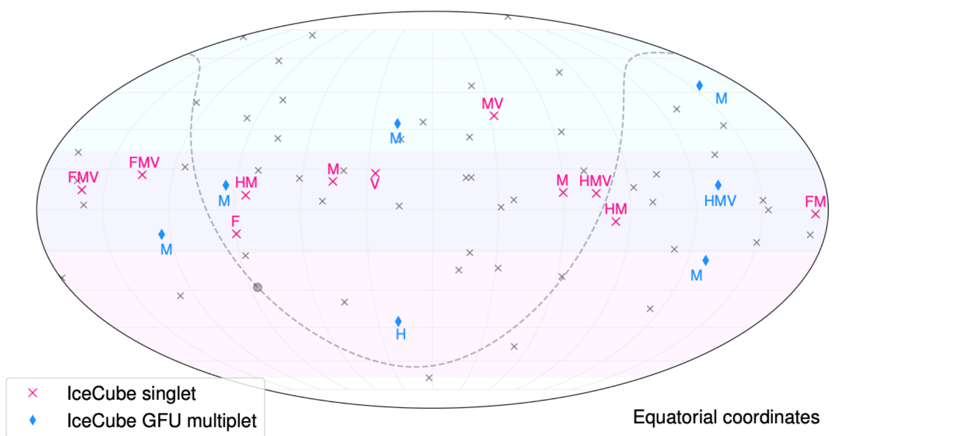

Figure 1: Sky map in equatorial coordinates showing IceCube alert positions observed by IACTs between October 2017 and January 2021 (in color, according to the alert type), and those not followed-up during the

Constant participation of HESS in muliwavelength Target of Opportunity observations of IceCube alerted events

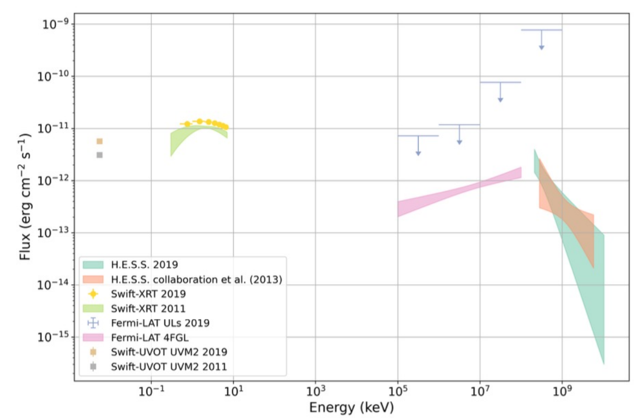

Figure 2: 1ES 1312-423 MWL SED showing archival data and observations obtained during the period following the GFU neutrino alert and contemporaneous to H.E.S.S. ToO observations.

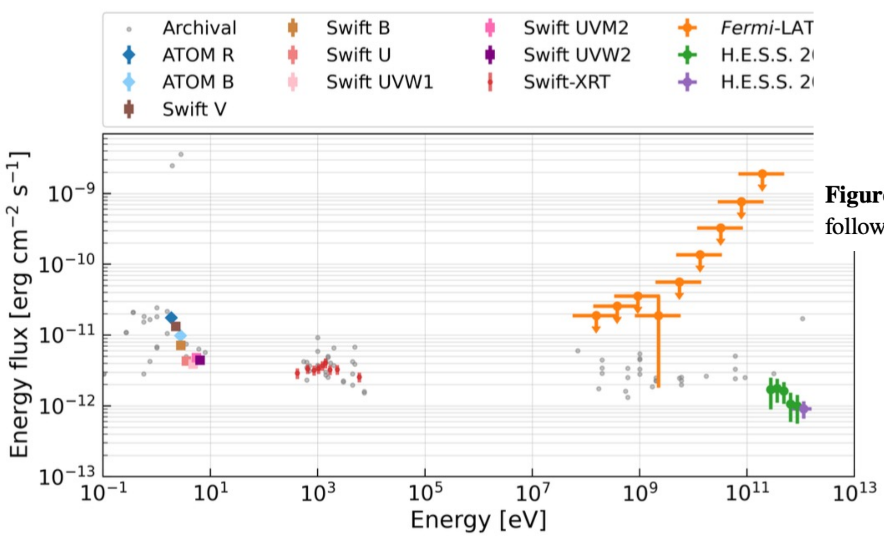

NO significant gamma-ray excess was detected in any case observed

Figure 1: SED of the blazar PKS 0625-35 using data from H.E.S.S., *Fermi*-LAT, *Swift*-XRT, and ATOM. Archival data is displayed in gray.

Multi-messenger observations – GW 170817

*Abbott et al. , ApJL **848**, L12 (2020)*

*H.E.S.S. Collaboration, ApJL **894**, L16 (2020)*

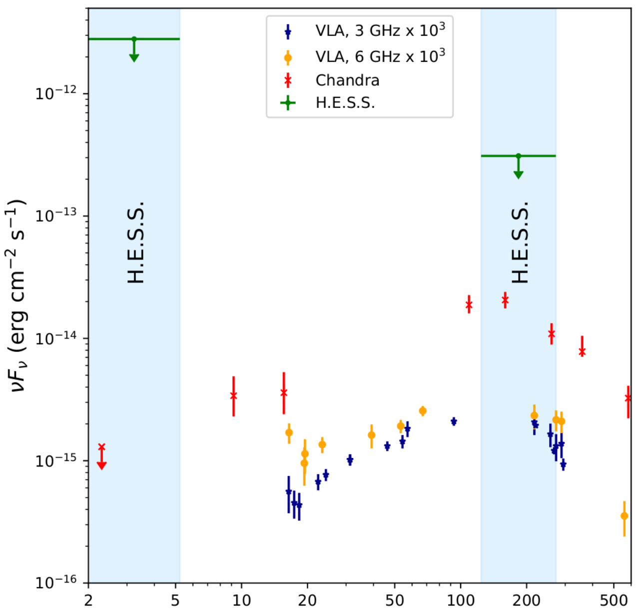

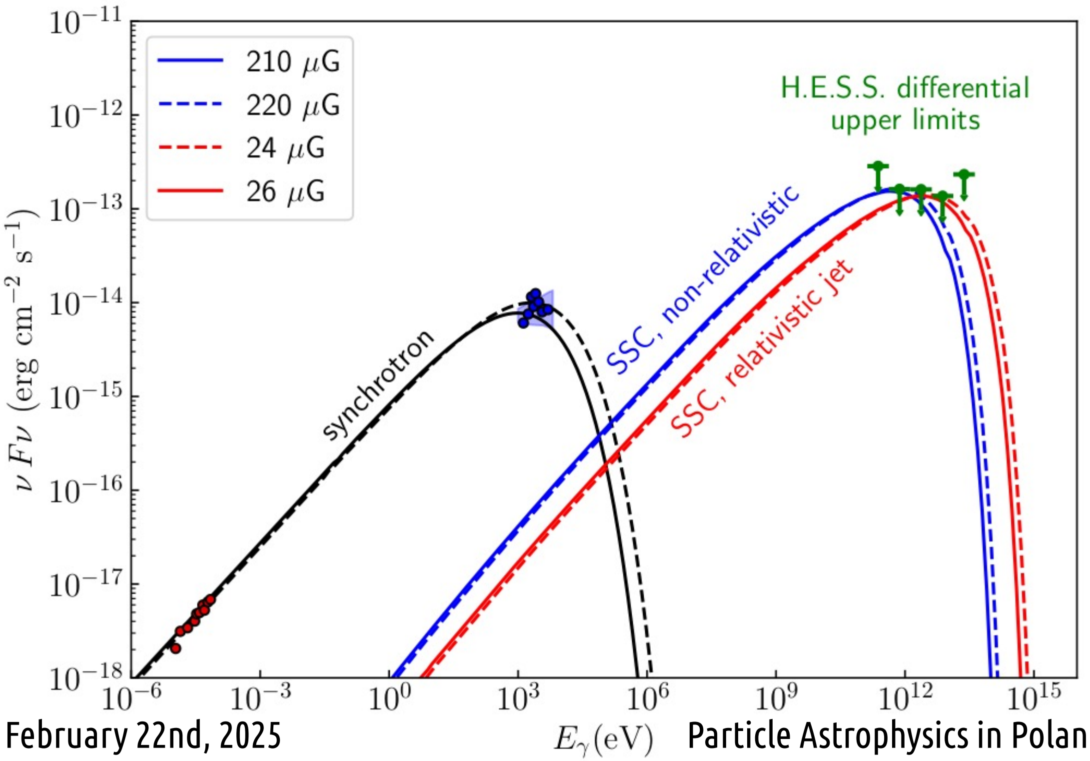

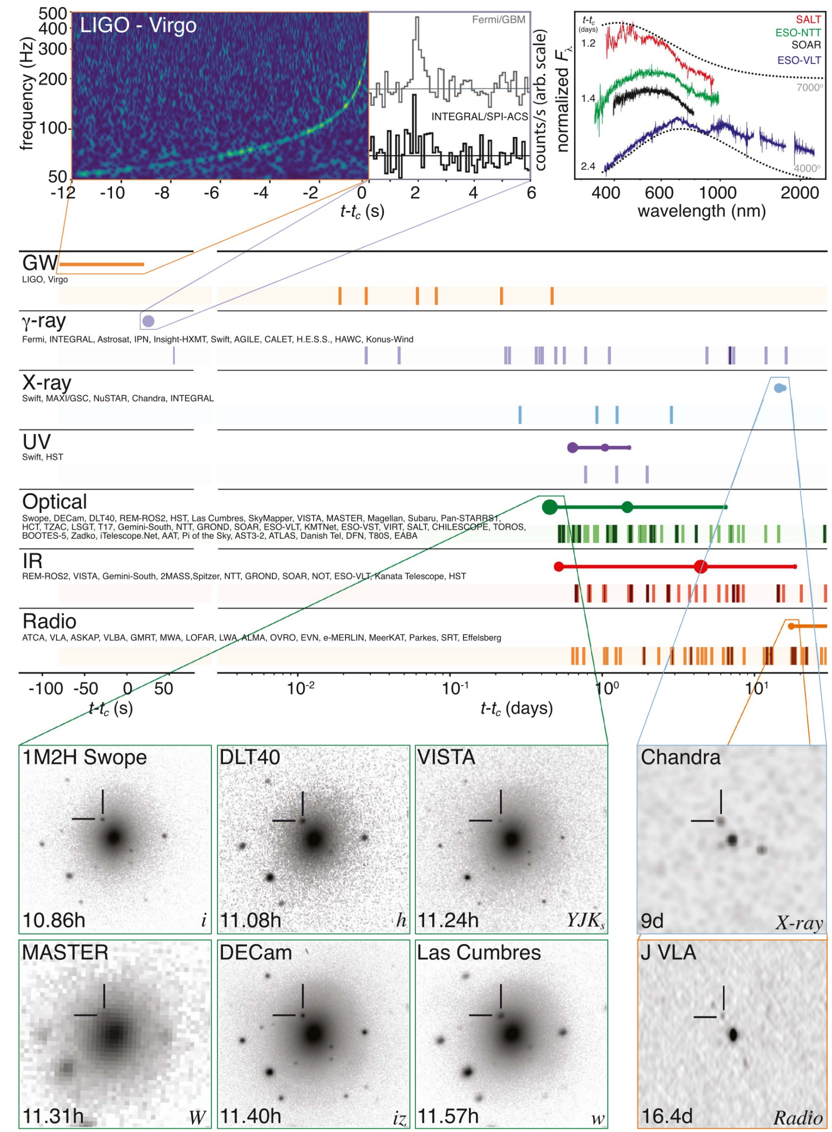

Search for γ-rays from annihilation of dark matter

H.E.S.S. Collaboration (2022)

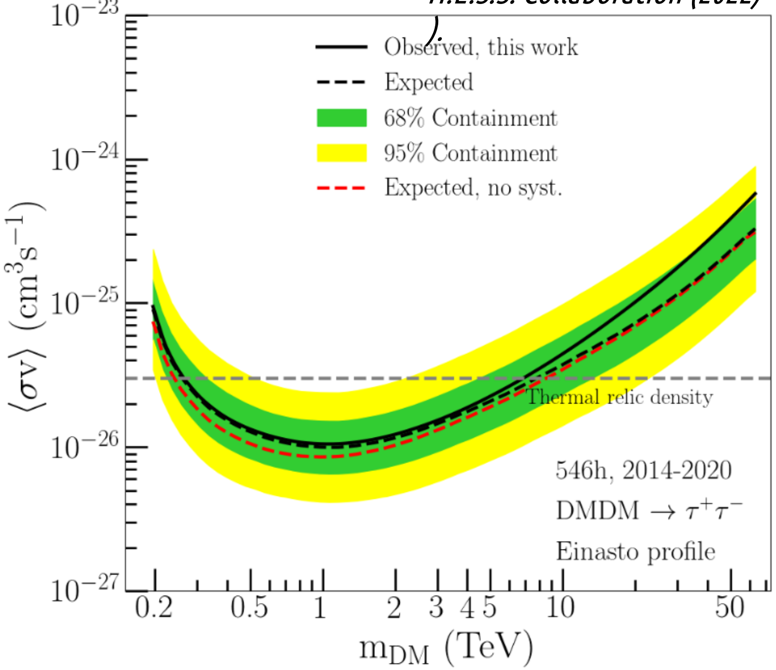

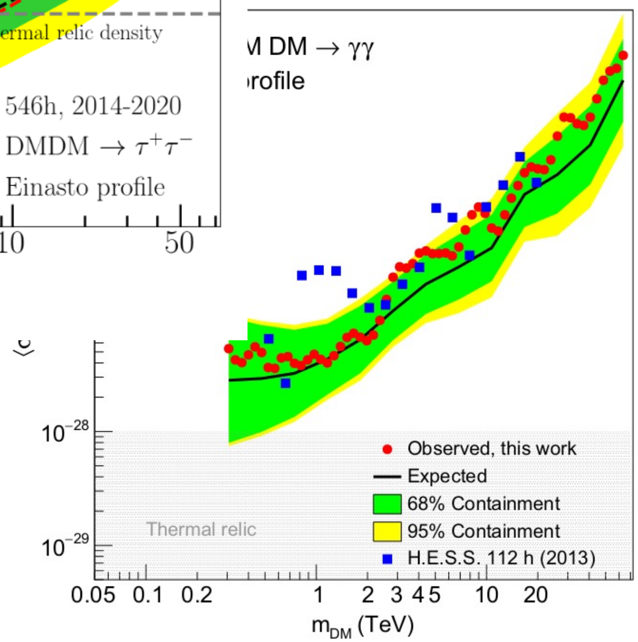

Rinchiuso for H.E.S.S. Collaboration (2021).

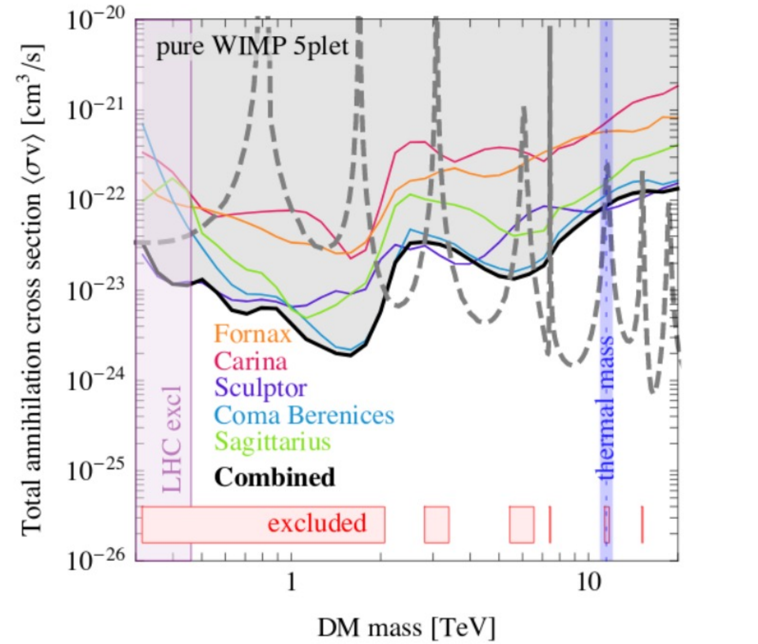

Figure 2. 95% C. L. upper limits on $\langle\sigma v\rangle$ as a function of $m_{\rm DM}$. *Left:* Limits for the *gamma-line* derived from H.E.S.S. observations taken over ten years (254 h live time) of the inner 300 pc of the GC region. Observed limits (red dots) and mean expected limit (black solid line) are shown together with the 1σ (green band) and 2σ (yellow band) containment bands. *Right:* Limits for the 5plet towards dwarf galaxies are shown for single galaxy observation and for their combination (black solid line). The predicted cross section (gray dashed line), thermal mass (blue band) and excluded masses (red boxes) are represented.

SUMMARY

– **H.E.S.S. still performs very well** in many aspects of particle astrophysics research with its scientific program contributing significantly to multi-wavelength and multi-messenger observations

– **systematic upgrades** (addition of CT5 telescope, mirror re-coating and camera upgrade) allow for improvement in the system performance

– H.E.S.S. is still the only **hybrid system** – a pathfinder for the Cherenkov Telescope Array (CTA) and a test bed for CTA technologies

– the **future of H.E.S.S. in “the CTA era”** is under constant discussion – currently being secured until **September 2028**

-- **legacy program** prepared to release data to the community